### Cosmic String Theory: The Current Status

Leandros Perivolaropoulos<sup>1</sup>,<sup>2</sup>

Center for Theoretical Physics Laboratory for Nuclear Science Massachussetts Institute of Technology Cambridge, Mass. 02139, USA.

#### Abstract

This is a pedagogical introduction to the basics of the cosmic string theory and also a review of the recent progress made with respect to the macrophysical predictions of the theory. Topics covered include, string formation and evolution, large scale structure formation, generation of peculiar velocity flows, cosmic microwave background (CMB) fluctuations, lensing, gravitational waves and constraints from the msec pulsar. Particular emphasis is placed on the signatures predicted on the CMB and the corresponding non-gaussian features.

Based on four lectures presented at the Trieste 1994 Summer School for Particle Physics and Cosmology. To appear in the School Proceedings.

<sup>&</sup>lt;sup>1</sup>E-mail address: leandros@mitlns.mit.edu

<sup>&</sup>lt;sup>2</sup>Also, Department of Physics, Brown University, Providence, R.I. 02912.

# Contents

1	Intr	oduction-Cosmology Basics	2	
<b>2</b>	Formation of Topological Defects			
	2.1	Kibble Mechanism	9	
	2.2	Non-local defects: Textures	12	
	2.3	Classical Field Theory	14	
3	Cosmic String Evolution		16	
	3.1	Nambu Action	16	
	3.2	Scaling Solution	19	
	3.3	Benefits of Scaling	20	
4	Gravitational Effects		22	
	4.1	String Metric: The Deficit Angle	22	
	4.2	Velocity Fluctuations		
	4.3	Microwave Background Fluctuations		
	4.4	Lensing		
5	Str	Structure Formation 28		
	5.1	Sheets of Galaxies, Filaments	28	
	5.2	Peculiar Velocities	33	
	5.3	Power Spectrum	34	
	5.4	Gravitational Radiation	36	
	5.5	A String Detection?	37	
6	Cosmic Strings and the Microwave Background		39	
	6.1	Angular Spectrum Basics	39	
	6.2	String Angular Spectrum		
	6.3	Statistical Tests		
7	Cor	nclusion	56	

# 1 Introduction-Cosmology Basics

The Big Bang theory[1] is the best theory we have for describing the universe. It is a particularly simple and highly successful theory. It makes three basic observationally consistent assumptions and derives from them some highly non-trivial predictions which have been verified by observations. The main assumptions are the following:

- The universe is a homogeneous and isotropic thermal bath of the known particles (cosmological principle [2]).
- General Relativity is the correct theory to describe physics on cosmological scales.
- The energy momentum tensor of the universe is well approximated by that of a perfect fluid *i.e.*

$$T_{ij} = diag[\rho, -p, -p, -p] \tag{1}$$

The first two assumptions imply that the universe can be described by the Robertson-Walker metric of the form

$$ds^{2} = dt^{2} - a(t)^{2} \left[ \frac{dr^{2}}{1 - kr^{2}} + r^{2} (d\theta^{2} - \sin^{2}\theta d\phi^{2}) \right]$$
 (2)

where a(t) is known as the scale factor of the universe and k can be normalized to the values -1, 0, 1 for an open (negative curvature), spatially flat and closed (positive curvature) universe respectively.

The third assumption can be used along with the Einstein equations to derive the Friedman equations that determine the dynamics of the scale factor a(t). These may be written as

$$\left(\frac{\dot{a}}{a}\right)^2 - \frac{k}{a^2} = \frac{8\pi G}{3}\rho\tag{3}$$

$$\frac{\ddot{a}}{a} = \frac{4\pi G}{3}(\rho + 3p) \tag{4}$$

These are two equations with three unknown functions  $(a(t), \rho(t), p(t))$  and therefore the equation of state  $p = p(\rho)$  is also needed in order to obtain a solution. For example, for a flat (k = 0) radiation dominated universe

 $(p = \rho/3)$ , it is easy to show that  $a(t) \sim t^{1/2}$  while for a matter dominated universe (p = 0) we have  $a(t) \sim t^{2/3}$ .

Observations indicate that at the present time the matter density dominates over radiation density in the universe  $(\rho_{mat}(t_0) \gg \rho_{rad}(t_0))$  and therefore we live in a matter dominated universe. However, this was not the case at early times. The Friedman equations may be used to show that

$$\frac{d}{da}(\rho a^3) = -3a^2p\tag{5}$$

which implies

$$\rho_{mat}(t) \sim a(t)^{-3} \tag{6}$$

$$\rho_{rad}(t) \sim a(t)^{-4} \tag{7}$$

and therefore there is a time  $t_{eq} < t_0$  of equal matter and radiation such that

$$t < t_{eq} \Rightarrow \rho_{mat}(t) < \rho_{rad}(t)$$
 (8)

Using Eq. (7) and the well known result from statistical mechanics that  $\rho_{rad} \sim T^4$  we obtain that the temperature of radiation scales as

$$T(t) \sim a(t)^{-1} \tag{9}$$

in a matter or radiation dominated universe. Cosmic Microwave Background (CMB) measurements[3] have shown that  $T(t_0) = 2.736 \pm 0.017$  and therefore the temperature at earlier times is predicted to be

$$T(t) = 2.7^{0} K \frac{a(t_0)}{a(t)} \tag{10}$$

The three main predictions of the Big Bang theory are the following:

- The expansion of the universe (Hubble's law).
- The existence of the Cosmic Microwave Background (CMB).
- The relative abundances of the light elements (nucleosynthesis).

A simple way to derive Hubble's law in the case of a flat (k=0) universe is to consider two points in space separated by coordinate (comoving) distance dr (with  $d\theta = d\phi = 0$ ). The proper (physical) distance between the two points is given by

$$ds = a(t)dr (11)$$

Therefore, the physical relative velocity between the two points is

$$\dot{s} = \dot{a}r + a\dot{r} \tag{12}$$

where  $\dot{a}r$  is known as the Hubble flow and  $a\dot{r}$  is the peculiar velocity. For large comoving distances r the second term can be ignored and we have

$$v = \dot{s} \simeq \frac{\dot{a}}{a} s \equiv H(t)s \Rightarrow cz \simeq v = H(t)s$$
 (13)

where z is the Doppler redshift and  $H(t) \equiv \frac{\dot{a}}{a}$  is the Hubble constant at cosmic time t. Eq. (13) is known as the Hubble's law[4] and has been verified by observations. The value of  $H(t_0)$  may be written as

$$H(t_0) = 100h \ km/(sec \cdot Mpc) \tag{14}$$

with  $h \in [1/2, 1]$ .

A particularly important prediction of the Big Bang theory is the existence of the CMB[5]. Penzias and Wilson[6] observed for the first time in 1965 a highly isotropic backgroung of microwave photons with spectrum that was thermal to a high accuracy. Several experiments since then have verified this observation and today it is known that the temperature of this background is given by Eq. (10)  $(t = t_0)$  and temperature anisotropies are of  $O(10^{-5})$ . An additional term of dipole anisotropy [7] is known to be present due to our motion with respect to the CMB. The magnitude of this term is  $\frac{\delta T}{T} \simeq 10^{-3}$  and corresponds to a velocity of the earth of about 600km/sec with respect to the CMB frame. Even though the dipole term dominates over the primordial fluctuations it can be easily subtracted due to its dipole nature.

CMB photons are free at the present time  $t_0$  (they have mean free path of cosmological scale) and there is no apparent mechanism that could have caused their thermalization. However, such mechanism is naturally provided by the Big Bang theory. According to this theory, the universe is

hotter at early times (cf Eq. (10)) and therefore there is a time  $t_{rec} < t_0$  (time of recombination) when photons are energetic enough to ionize matter  $(T(t_{rec}) \gtrsim T_{ion} \simeq O(10^4)^{0} K)$ . In such a primordial plasma, thermalization of photons can occur effectively[8, 9].

The redshift  $z(t_{rec})$  at the time of recombination defined as

$$1 + z(t_{rec}) \equiv \frac{a(t_0)}{a(t_{rec})} = \frac{T(t_{rec})}{T(t_0)}$$
 (15)

is therefore  $z(t_{rec}) \simeq 1500$ . Thus, according to the Big Bang theory the CMB photons were scattered for last time at  $t=t_{rec}$  and carry a 'photograph' of the universe taken when it was 1500 times smaller and hotter. There is exciting information hidden in this map. An as yet unknown source has created primordial fluctuations that evolved gravitationally into what we see as galaxies, clusters and large scale structure today. It is those fluctuations in their primordial gravitationally unaffected form that have been recorded by the CMB photons. Clearly, information on such a primordial pattern can impose severe constraints on theories attempting to explain the origin of primordial fluctuations.

The third prediction of the Big Bang theory is made on the relative cosmological abundances of the light elements  $(H, He, H^3, Li^7)$  which span 10 orders of magnitude and are predicted correctly by the Big Bang theory provided that the baryon to photon ratio is  $\eta \equiv \frac{n_B}{n_\gamma} \simeq 10^{-10} [10]$ .

The assumptions of homogeneity and isotropy made by the Big Bang theory, even though consistent with very large scale ( $\gtrsim 100h^{-1}Mpc$ ) observations[11] are only first approximations to the realistic system. It is enough to look at the night sky to realize that the universe is not homogeneous and isotropic on relatively small scales. Instead, matter tends to cluster gravitationally and form well defined structures. In fact, detailed large scale structure observations have indicated the existence of *sheets* and *filaments* of galaxies separated by large voids. The typical scale of these structures is about  $50h^{-1}Mpc$  [12, 13, 14, 15].

Fig. 1 shows a slice of the CfA survey which is a map of galaxies in redshift space (depth in the sky). The presence of the above described structures is evident in this map (the axis of redshifts can easily be converted to distance (depth in the sky) by using Hubble's law<sup>3</sup>). Can these large structures be

<sup>&</sup>lt;sup>3</sup>For example for h = 1 dividing z by 100 gives the corresponding distance in Mpc.

explained by assuming that matter moved due to gravity from an initially homogeneous state?

**Figure 1:** The CfA Survey shows a map of galaxies in redshift space (depth in the sky). This 'slice of the universe' includes a range of about 6<sup>o</sup> in declination space.

The maximum distance that matter can have travelled since the Big Bang is

$$\delta r_{max} \simeq \delta v \ t_0 \simeq 6h^{-1}Mpc$$
 (16)

where  $\delta v \simeq 600 km/sec$  is the typical peculiar velocity of galaxies (induced by gravity) at the present time  $t_0$ . This  $\delta r_{max}$  is much less than the typical scale of observed structures. Thus, these structures can not be the result of gravity alone. They must also reflect the presence of primordial perturbations. The question that we want to address is What caused these fluctuations?

Until about 15 years ago there was no physically motivated mechanism to cause these perturbations. However, during the past decade, two classes of theories motivated from quantum field theory have emerged and attempt to give physically motivated answers to the question of the origin of structure in the universe.

A model for large scale structure formation is characterized by two basic features. The first is the kind of the assumed dark matter and the second is the type of primordial fluctuations.

Dynamical measurements based mainly on peculiar velocities have shown that at least 90% of the matter in the universe is not luminus [16, 17, 18]. This non-luminus matter which has not been directly detected yet, is called dark matter and its properties determine critically the rate of gravitational growth of primordial perturbations at different cosmic epochs. In particular, dark matter with low non-relativistic velocities at the time  $t_{eq}$  (when fluctuations start to grow) is called cold dark matter (CDM)[19]. A CDM candidate motivated from particle physics is the hypothetical particle axion[20] which appears to be a necessary consequence of a successful resolution of the strong CP problem in QCD. Dark matter which has relativistic velocities at  $t_{eq}$  is called hot dark matter (HDM) and a primary candidate for it is a massive  $(25h^{-2}eV)$  neutrino. Due to their relativistic velocities HDM particles can not cluster gravitationally at early times and small scales. This effect is called free streaming[21]. The critical scale for HDM perturbation growth is the free streaming scale  $l_{fs}(t) \simeq v_{\nu}(t)t$  i.e. the distance travelled by a HDM particle in a Hubble time t. Adiabatic perturbations (those produced by inflation) on scales  $l < l_{fs}$  are erased on small (galactic) scales due to the effects of free streaming.

The second characteristic of large scale structure formation models is the type of primordial fluctuations. There are two broad classes of primordial perturbations, both produced by physically motivated mechanisms. The first includes gaussian adiabatic perturbations produced [22, 23, 24, 25] during a period of exponential growth of the universe known as *inflation* [26]. These perturbations may be represented as a superposition of plane waves with random phases *i.e.* 

$$\delta \equiv \frac{\delta \rho}{\rho}(x) \sim \sum_{k} |\delta_k| e^{i\theta_k} e^{ikx} \tag{17}$$

where  $\frac{\delta \rho}{\rho}(x)$  represents the primordial density fluctuation pattern and  $\theta_k$  are random uncorrelated phases. By the central limit theorem, since  $\delta$  is a superposition of an infinite number of uncorrelated random variables, its probability distribution is gaussian *i.e.* 

$$P(\delta) \sim e^{-\delta^2/\sigma^2} \tag{18}$$

Fig. 2a shows schematically the features of such a gaussian perturbation pattern.

**Figure 2:** Gaussian fluctuations may be represented as a superposition of plane waves with random phases (a) while topological defect fluctuations are represented by a superposition of seed functions (b).

The second class includes primordial perturbations produced by a superposition of localized seeds created during a phase transition in the early universe. Such seeds are known as topological defects[27, 28, 29, 30, 31] and their formation is predicted by many (but not all) Grand Unified Theories (GUTs)[32]. The pattern of topological defect perturbations may be represented as a superposition of localized functions (Fig. 2b) *i.e.* 

$$\delta = \sum_{i} \frac{\delta \rho}{\rho} (x - x_i) \tag{19}$$

and therefore, in general the probability distribution of  $\delta$  is not gaussian<sup>4</sup>)

Both inflationary and topological defect perturbations can be combined with either HDM or CDM for the construction of structure formation theories. In models based on gaussian adiabatic fluctuations with HDM, galactic scale fluctuations are erased by free streaming and therefore these structures can only form at later times by fragmentation of larger objects. This is in contrast with observations indicating that galaxies formed earlier than larger

<sup>&</sup>lt;sup>4</sup>For a not very large number of superposed seeds.

structures. These models face also other conflicts with observations (eg they violate CMB fluctuation constraints) and have therefore been placed into disfavor. On the other hand, the model based on inflationary gaussian fluctuations with CDM has been well studied and makes concrete predictions that are in reasonable agreement with most types of observations especially on small and intermediate scales. This model is currently the 'standard model' for structure formation[33].

Models based on topological defect perturbations combined with either hot or cold dark matter have not been as well studied but they have been shown to have several interesting features that make them worth of further investigation. Most of the remaining of these talks will focus on one of the most interesting types of topological defects cosmic strings[34, 35]. Three basic aspects of cosmic string physics will be discussed: their formation, evolution and gravitational effects.

# 2 Formation of Topological Defects

#### 2.1 Kibble Mechanism

Even though no particle corresponding to a scalar field has been discovered so far, the role of scalar fields in particle physics models is central. Indeed, scalar fields provide a natural and simple mechanism to induce spontaneous symmetry breaking in gauge theories thus achieving two important goals: First maintain gauge invariance and renormalizability of these theories and second give mass to gauge bosons thus making them consistent with inducing short range interactions like the strong and electroweak forces. Symmetry breaking can be achieved by the use of scalar field potentials of the form

$$V(\Phi) = \frac{\lambda}{4} (\Phi^{\dagger} \Phi - \eta^2)^2 \tag{20}$$

where  $\Phi = [\Phi_1, ..., \Phi_N]$  is a multiplet of scalar fields.

Figure 3: The Kibble Mechanism: The evolution of a scalar field in a potential with discrete minima ((a) left) leads to the formation of a domain wall in physical space after the relaxation of the field in its minima ((a) right). When the potential minimum (vacuum manifold) has the topology of a circle  $(S^1)$  a cosmic string forms in physical space (b) while a monopole forms when the vacuum manifold is a sphere  $(S^2)$  (c).

Consider for example a one component scalar field whose dynamics is determined by the double well potential of Fig. 3a. At early times and high temperature T the field  $\Phi$  will have enough energy to span the whole range of the potential<sup>5</sup> and go over the barrier between the two minima. As the universe cools and expands however, the energy of the scalar field will drop

<sup>&</sup>lt;sup>5</sup>The temperature dependence of the effective potential is ignored here since its calculation is highly non-trivial in out of equilibrium systems like the one discussed here.

and it will eventually be confined in one of the two minima  $(+\eta, -\eta)$ . The choice of the minimum is arbitrary. In fact, there will be neighbouring uncorrelated or causally disconnected regions where the choice of the minimum (vacuum) will be opposite (Fig. 3a). By continuity of the field  $\Phi$  there will be a surface separating the two domains where  $\Phi = 0$  and therefore  $\Phi$  will be associated with the high energy of the local potential maximum. This surface of trapped energy density is known as a domain wall and is the simplest type of topological defect. Domain walls form in theories where the vacuum manifold M (minimum of potential) has more than one disconnected components. This fact is expressed in homotopy theory[36] as  $\pi_0(M) \neq 1$ .

The mechanism described above for the formation of domain walls is known as the Kibble mechanism[27, 28] and applies in a similar way to the case of other topological defects. Consider for example the case where the dynamics of a two component scalar is determined by the potential of Fig. 3b. After the field relaxes to its vacuum, there will be (by causality) regions of the universe where the field  $\Phi$  will span the whole vacuum manifold as we travel around a circle in physical space. Topologically stable vortices can also form in systems with multiple scalars [37] while metastable vortices can even form in systems where the vacuum manifold is not  $S^1$ . In the later cases the stability is not topological by dynamical [38]. By continuity of  $\Phi$  there will be a point inside this circle where  $\Phi = 0$ . Such a point (and its neighbourhood) will be associated with high energy density due to the local maximum of the potential at  $\Phi = 0$ . By extending this argument to three dimensions, the point becomes a line of trapped energy density known as the *cosmic string*. In general cosmic strings form in field theories where there are closed loops in the vacuum manifold M that can not be shrank to a point without leaving M. In homotopy theory terms, we require that the first homotopy group of the vacuum should be non-trivial i.e.  $\pi_1(M) \neq 1$ . It may be shown that this is equivalent to  $\pi_0(H) \neq 1$  where H is the unbroken group in the symmetry breaking  $G \to H$  (M=G/H). As will be discussed below, the number of times the field  $\Phi$  winds around the vacuum manifold as we span a circle in physical space around the string is a topologically conserved quantity called the topological charge (or winding number) and its conservation guarantees the stability of the string.

In theories where the vacuum manifold is a sphere, the defect that forms by the Kibble mechanism is pointlike and is known as the *monopole* (Fig. 3c). In general monopoles form in theories where the vacuum manifold has

unshrinkable spheres i.e.  $\pi_2(M) \neq 0$  (equivalent to  $\pi_1(H) \neq 1$ ). Monopoles, like strings have associated topological charge whose conservation guarantees their stability. As will be discussed later, most types of domain walls and monopoles are inconsistent with the standard Big Bang theory as they lead to quick domination of the universe by defect energy and subsequent early collapse. On the other hand, in the case of strings there is a natural mechanism to effectively convert string energy to radiation and thus prevent the string network from dominating the universe.

Topological defects similar to the ones described above can form not only in a cosmological setup but also in several condensed matter systems [39] like liquid crystals[40],  $He^3$  [41] and superconductors[42].

#### 2.2 Non-local defects: Textures

All the defects discussed so far have two important properties:

- The field configuration can not be continuously deformed to the trivial zero energy vacuum where the field would point to the same direction everywhere in space.
- There is a well defined region in space where most of the defect energy is localized. It will be shown that the size of this domain is proportional to the inverse of the symmetry breaking scale  $\eta$ .

From the second property it follows that the above described defects are *localized defects*. There is a second class of defects that have the first but not the second of the above properties. *Textures* belong to this later class[43, 44].

**Figure 4:** The field configuration of a non-local *texture* in one (a) two (b) and three (c) space dimensions.

Consider a global (no gauge fields) theory where the vacuum manifold is  $S^1$  (a circle). Consider also the one dimensional (fixed boundary conditions) scalar field configuration shown in Fig. 4a. This configuration is topological (can not be deformed to the trivial vacuum) but is non-local (there is no core of energy density). It is known as the one dimensional texture and in general it is non-static. It is straightforward to generalize the one dimensional texture to two dimensions and three dimensions by considering theories with  $M = S^2$  and  $M = S^3$  (Fig. 4b and 4c). In fact it may be shown (Derrick's theorem[45, 46]) that a rescaling of the radial coordinate r by a scale factor  $\alpha > 1$   $(r \to \alpha r)$  leads to a rescaling of the energy of the three dimensional texture by the inverse factor  $\alpha$  ( $E \to E/\alpha$ ) which implies that collapse and subsequent unwinding is an energetically favored process provided that the topological charge is larger than a critical value[47, 48, 49, 50]. Even though the physics and observational effects of textures are particularly interesting[51, 52, 53, 54] subjects they are outside of the scope of this review and will not be further

discussed here (for a good review of textures see Ref. [55]).

### 2.3 Classical Field Theory

In what follows I will focus on the cosmological effects of cosmic strings. The simplest model in which strings involving gauge fileds can form [56] is the Abelian Higgs model involving the breaking of a U(1) gauge symmetry. The Lagrangian of the Abelian Higgs model is of the form

$$\mathcal{L} = \frac{1}{2} D_{\mu} \Phi D^{\mu} \Phi - V(\Phi) + \frac{1}{4} F_{\mu\nu} F^{\mu\nu}$$
 (21)

where  $F_{\mu\nu} = \partial_{\mu}A_{\nu} - \partial_{\nu}A_{\mu}$ ,  $D_{\mu} \equiv \partial_{\mu} - ieA_{\mu}$  and  $V(\Phi) = \frac{\lambda}{4}(|\Phi|^2 - \eta^2)^2$ ,  $(\Phi = \Phi_1 + i\Phi_2)$ . The field configuration corresponding to a string[56, 46] in this theory is shown in Fig. 3b. The topological stability of the string (vortex in two space dimensions) is due to the conservation of the topological invariant (topological charge or winding number)

$$m = \int_0^{2\pi} \frac{d\alpha}{d\theta} d\theta \tag{22}$$

where  $\alpha$  is an angular variable determining the orientation of  $\Phi$  in the vacuum manifold which is  $S^1$  (circle) in the Abelian Higgs model and  $\theta$  is the azimouthal angle around the vortex in physical space. For the string shown in Fig. 3b we have m=1 and the field winds once in the positive direction as we span a circle around the string.

The field configuration of a vortex may be described by the following ansatz:

$$\Phi = f(r)e^{im\theta} \tag{23}$$

$$\vec{A} = \frac{v(r)}{r}\hat{e}_{\theta} \tag{24}$$

with f(0) = v(0) = 0,  $f(\infty) = \eta$  and  $v(\infty) = m/e$ . The forms of f(r) and v(r) can be obtained numerically[56] from the field equations with the above ansatz. The energy of the vortex configuration (energy of string per unit length) is

$$\mu = \frac{E}{L} = \int d^2x (f'^2 + \frac{v^2}{r^2} + \frac{(ev - m)^2}{r^2} f^2 + \frac{\lambda}{4} (f^2 - \eta^2)^2)$$
 (25)

Clearly,  $v \neq 0$  is required for finite energy *i.e.* the gauge field is needed in order to screen the logarithmically divergent energy coming from the angular gradient of the scalar field. A vortex with no gauge fields is known as a global vortex and its energy per unit length diverges logarithmically with distance from the string core. This divergence however is not necessarily a problem in systems where there is a built-in scale cutoff like systems involving interacting vortices. In such systems the intervortex distance provides a natural cutoff scale for the energy integral. Similar considerations apply to monopoles with no gauge fields even though the energy divergence in that case is linear rather than logarithmic [57, 58, 59]

Even though no analytic solution has been found for the functions f(r) and v(r) it is straightforward to obtain the asymptotic form of these functions from the field equations (Nielsen-Olesen equations). The obtained asymptotic form for  $r \to \infty$  is [56, 46] (but see Ref. [60] for a correction to the standard result)

$$f(r) \rightarrow \eta - \frac{c_f}{\sqrt{r}} e^{-\sqrt{\lambda}\eta r}$$
 (26)

$$v(r) \rightarrow \frac{m}{e} - c_v \sqrt{r} e^{-e\eta r}$$
 (27)

where  $c_v$  and  $c_f$  are constants. Therefore the width of the vortex is

$$w \sim \eta^{-1} \tag{28}$$

where  $\eta$  is the parameter of the symmetry breaking potential also known as the scale of symmetry breaking. The energy per unit length  $\mu$  may also be approximated in terms of  $\eta$  as

$$\mu \simeq \int_{w} d^2x V(0) \sim \eta^2 \tag{29}$$

The typical symmetry breaking scale for GUTs is  $\eta \simeq 10^{16} GeV$  which leads to extremely thin and massive strings

$$w \simeq 10^{-30} cm \tag{30}$$

$$\mu \simeq 10^{14} tons/mm \tag{31}$$

Therefore, the Nielsen-Olesen vortex may be viewed as a linear, topologically stable field configuration involving both magnetic field energy and

Higgs potential energy that decay exponentially at large distances. No finite gauge transformation can gauge away a vortex gauge field everywhere in space. The several interesting quantum field theoretical interactions of vortices with particles (fermions) are out of the scope of this review[61].

# 3 Cosmic String Evolution

#### 3.1 Nambu Action

The exact analytic treatment of the evolution of a network of strings would involve the analytic solution of the time dependent nonlinear field equations derived from the Lagrangian of Eq. (21) with arbitrary initial conditions. Unfortunately no analytic solution is known for these equations even for the simplest nontrivial ansatz of the static Nielsen-Olesen vortex. Even the numerical solution of these equations is practically impossible for systems of cosmological scales and with complicated initial conditions. The obvious alternative is to resort to realistic approximations in the numerical solution of the field equations in cosmological systems. First, the correct initial conditions for a numerical simulation must be obtained by simulating the above described Kibble mechanism on a lattice. This may be achieved by implementing a Monte-Carlo simulation implemented first by Vachaspati and Vilenkin [62]. They considered a discretization of the vacuum manifold  $(S^1)$ into three points (Fig. 5) and then assigned randomly these three discrete phases to points on a square lattice in physical space in three dimensions. For those square plaquettes for which a complete winding of the phase in the vacuum manifold occured, they assigned a string segment passing through. It may be shown that this algorithm leads to strings with no ends within the lattice volume i.e. strings either form loops or go through the entire lattice volume (infinite strings). This simulation showed that the initial string network consists of 80% long strings and 20% loops.

**Figure 5:** The Vachaspati-Vilenkin algorithm used to study the formation of a string network by Monte-Carlo simulations.

In order to find the cosmological effects of this initial string network, it must be evolved in time. Since it is impractical to evolve the full field equations on the vast range of scales  $10^{-30}cm$  (string width) to  $10^3Mpc$  (largest cosmological scales) we must resort to some approximation scheme. The ratio w/R of the width of the string over the string coherence scale is an intrinsically small parameter for cosmological strings ( $w/R << 10^{-30}$  for  $t > t_{eq}$ ). Thus, this parameter can be used to develop a perturbation expansion[63, 64] for the action that describes the dynamics of a string segment. The zeroth order approximation is obtained for w/R = 0.

A heuristic derivation of the action of a zero width string may be obtained by using the analogy with a relativistic free point particle with mass m and velocity v. The relativistic action describing the motion of such a particle is of the form

$$S = -m \int_{A}^{B} d\tau = -m \int_{A}^{B} dt (1 - v^{2})^{1/2} \simeq \int_{A}^{B} dt (\frac{1}{2}mv^{2}) + const$$
 (32)

where A, B are the endpoints of the trajectory and  $\tau$  is the particle's proper time. As shown in Eq. (32), the non-relativistic limit is obtained for low velocities.

The trajectory of the string is not parametrized by only one variable (the proper time  $\tau$ ) but by two variables (a timelike variable  $\tau$  and a spacelike variable l which may be viewed as parametrizing the length of the string). Thus, the generalization of the point particle relativistic action to the string with mass per unit length  $\mu$  is the Nambu action defined as:

$$S = -\mu \int_{A}^{B} dl d\tau \sqrt{-g^{(2)}} + O(w/R)$$
 (33)

where  $g^{(2)} = det(X^{\mu}_{,a}X^{\nu}_{,b}g_{\mu\nu})$   $(a,b=1,2\to(\tau,l),~\mu,\nu=1,...4)$  is the metric of the world sheet spanned by the string. The Nambu action is an excellent approximation to the dynamics of non-intersecting cosmic string segments and is much simpler to handle numerically than the full field theoretic action.

**Figure 6:** The intercommutation (exchange of string segments) occurs when string segments intersect and favors formation of string loops (a). The effect is closely related to the right angle scattering of vortices in head on collisions (b,c) (from Ref. [67]).

A crucial assumption in the derivation of the Nambu action is that string segments do not interact with each other. This assumption breaks down when two string segments intersect. The outcome of such an event can only be found by evolving the full field equations. Such numerical experiments have shown [65, 66, 67] that at intersections string segments exchange parteners

and a process known as intercommuting occurs (Fig. 6a). Intercommuting is closely related to the right angle scattering of vortices in head on collisions (Fig. 6b,c) which has been observed in several numerical experiments and can be analytically understood using dynamics in moduli spaces[68]. As shown in Fig. 6a intercommuting tends to favor the formation of string loops which oscillate and decay by emitting gravitational radiation with characteristic frequency  $\omega \sim R^{-1}$  (R is the loop radius) and rate  $\dot{E} = \gamma G \mu^2$  ( $\gamma = const \simeq 50$ )[69].

Therefore, this mechanism for loop formation, provides also an efficient way for converting long string energy that redshifts with the universe expansion as  $E_{str} \sim a^{-2}$  to radiation energy that redshifts as  $E_{rad} \sim a^{-4}$ . This is the crucial feature that prohibits strings from dominating the energy density of the universe during the radiation era and makes the cosmic string theory a viable theory for structure formation in the universe.

#### 3.2 Scaling Solution

Using the Monte-Carlo initial conditions described above, the Nambu action to evolve string segments and intercommuting to describe intersection events, it is straightforward (though not easy) to construct numerical simulations describing the evolution of the string network in an expanding universe. Using this approach it has been shown [70] that the initial string network quickly relaxes in a robust way to a scale invariant configuration known as the scaling solution. According to the scaling solution the only scale that characterizes the string network is the horizon scale at any given time. On scales larger than the causal horizon scale t, the network consists of a random walk of long strings which are coherent on approximately horizon scales. On scales smaller than the horizon more recent simulations [71, 72, 73] (Fig. 7) have shown that the network consists of a fixed number of approximately 10 long strings coherent on horizon scales and a large number of tiny loops with typical radius  $10^{-4}t$ . The efficient formation of tiny loops by the intercommuting of long strings on small scales leads to the existence of wiggles on the long strings (wiggly strings). The effective mass per unit length of wiggly strings is larger than the bare mass  $(\mu_{eff} \simeq 1.4\mu)$  and their tension is smaller than the bare tension. The main features of wiggly strings [74, 75, 76, 77] are discussed in more detail below.

**Figure 7:** The string network in the matter era. The volume of the cube is  $(H/2)^3$  and the simulation box was plotted after an expansion by a factor a = 16 (from Ref. [71]).

There is a simple heuristic way to understand why does the network of strings approach a scaling solution with a fixed number of long strings per horizon scale. Consider for example the case when the number of long strings per horizon increases drastically. This will inevitably lead to more efficient intercommuting and loop formation thus transfering energy from long strings to loops and reducing the number of long strings per horizon back to its equilibrium value. Similarly if the number of long strings decreases reduced intercommuting and loop formation will tend to increase the number of long strings towards an equilibrium value. These heuristic arguments have been put in more detailed form using differential equations in Ref. [29].

### 3.3 Benefits of Scaling

The scaling behavior described above is a crucial feature of cosmic strings. It ensures that the string energy density remains a fixed fraction of the matter density and thus an overclosure and premature collapse of the universe is avoided. To see this we may calculate the total energy in long strings at a time t assuming a fixed number of M long strings per horizon volume. The

energy density of strings is

$$\rho_{str} \sim \frac{M\mu t}{t^3} \sim \frac{\mu}{t^2} \sim G\mu \rho_c \tag{34}$$

where I used the definition of the critical density  $\rho_c \sim (\frac{\dot{a}}{a})^2$  (see Eq. (3) with k=0). Eq. (34) implies that

$$\frac{\rho_{str}}{\rho_c} \simeq G\mu \simeq 10^{-6} \tag{35}$$

for  $\eta=10^{16} GeV$ . Therefore the density in strings remains a small fixed fraction of the energy density of the universe. As will be seen, this nice feature is not shared by domain walls even if it is assumed that walls approach a scaling solution.

Gauge monopoles and domain walls are inconsistent with standard cosmology each for a different reason. In the case of gauge monopoles there is no long range interaction and therefore there is no efficient mechanism to convert energy from monopoles into radiation. The monopole-antimonopole anihilation for example is very inefficient without long range interactions. Therefore, during the radiation era monopole energy redshifts with radiation as  $\rho_{mon} \sim a^{-3}$  and  $\frac{\rho_{mon}}{\rho_{rad}}$  scales as a(t) leading to  $\rho_{mon}(t_0) >> \rho_c(t_0)$  and a premature collapse of the universe[78].

If Grand Unification to a simple group is realized in nature, the formation of monopoles is inevitable. This is the well known monopole problem of standard cosmology and may be seen as follows: Consider the symmetry breaking  $G \to H$  of a simple GUT simple group G to a group H. In any realistic theory, H must include the gauge group of electromagnetism  $U(1)_{em}$  since it is an experimental fact that the photon is massless and therefore  $U(1)_{em}$  is unbroken. Now, the vacuum manifold at the broken symmetry phase is M = G/H. The homotopy sequence of homotopy theory may be used to show that

$$\pi_2(G/H) = \pi_1(H) = \pi_1(U(1)_{em}) = Z$$
 (36)

and therefore since  $\pi_2(M) \neq 1$  monopoles must form in GUTs.

The dilution of the monopole density during an epoch of exponential expansion of the universe (inflation) provides one solution to the monopole problem [26]. An alternative [79] solution is provided by constructing GUT

models where monopoles get temporarily connected by  $U(1)_{em}$  strings during a temporary breaking of electromagnetism. Such models have the disadvantage of being somewhat unatural by introducing extra phase transitions in the symmetry breaking sequence of GUTs.

GUT domain walls are inconsistent with standard cosmology[80] even if they manage to achieve a scaling solution. Consider for example a domain wall network with a single wall spanning each horizon scale. The wall energy density may be easily found as

$$\rho_w \sim \frac{V(0)\eta^{-1}t^2}{t^3} \sim \eta^3 t^{-1} \sim \frac{(G\eta^2)\eta t}{Gt^2}$$
 (37)

Thus for  $t = t_0$  and  $\eta \simeq 10^{16} GeV$  we obtain

$$\frac{\rho_w}{\rho_c}(t_0) \simeq 10^{52}$$
 (38)

The wall symmetry breaking scale must be at least 17 orders of magnitude smaller than the GUT scale for a model containing walls to be viable without inflation.

The above discussion shows the unique attractive features of cosmic strings compared to other defects in the context of standard cosmology. Several other such features will be discussed in the rest of this review.

# 4 Gravitational Effects

# 4.1 String Metric: The Deficit Angle

The most important interaction on cosmological scales is gravity. It is therefore important to understand the gravitational effects of strings before attempting to study in more detail their cosmological effects. The straight string solution is thin, cylindrically symmetric and Lorentz invariant for boosts along the length of the string. This imposes the following constraint on components of the energy momentum tensor  $T_{\mu\nu}$ 

$$T_z^z(\rho) = T_0^0(\rho) \simeq \mu \delta(x)\delta(y) \tag{39}$$

Also

$$T^{\nu}_{\mu,\nu} = 0 \Rightarrow \frac{d}{dx} T^x_x(\rho) = 0 \Rightarrow T^x_x = T^y_y = 0$$
 (40)

where use was made of the cylindrical symmetry and of the fact that  $T_x^x = T_y^y \to 0$  as  $r \to \infty$ . Therefore, the string energy momentum tensor may be approximated by

$$T_{\mu\nu} \simeq \delta(x)\delta(y)diag(\mu, 0, 0, -\mu) \equiv diag(\rho, p_x, p_y, p_z)$$
 (41)

which implies that the string has significant negative pressure (tension) along the z direction i.e.

$$p_z = -\rho = -\mu \qquad p_x = p_y = 0 \tag{42}$$

This form of  $T_{\mu\nu}$  may be used to obtain the Newtonian limit for gravitational interactions of strings with matter. For the Newtonian potential  $\Psi$  we have

$$\nabla^2 \Psi = 4\pi G(\rho + \sum_i p_i) = 0 \Rightarrow \vec{F}_N = 0 \tag{43}$$

and a test particle would feel no force by a nearby motionless straight string. Simulations have shown however that realistic strings are neither straight nor motionless. Instead they have small scale wiggles and move with typical velocities of  $v_s \simeq 0.15c$  coherent on horizon scales. What is the energy momentum tensor and metric of such wiggly strings?

The main effect of wiggles on strings is to destroy Lorentz invariance along the string axis, to reduce the effective tension and to increase proportionaly the effective mass per unit length of the string. Thus, the energy momentum tensor of a wiggly string is

$$T_{\mu\nu} \simeq \delta(x)\delta(y)diag(\mu_{eff}, 0, 0, -T)$$
 (44)

with  $T \equiv -p_z < \mu$ ,  $\mu_{eff} > \mu$  and  $\mu_{eff}T = \mu^2$  [77] ( $\mu$  is the 'bare' mass per unit length obtained from the field Lagrangian). As expected the above  $T_{\mu\nu}$  reduces to the straight string case for  $\mu_{eff} = T$ . The breaking of Lorentz invariance by the wiggles also induces a non-zero Newtonian force between the wiggly string at rest and a test particle since the tension (negative pressure) is not able to completely cancel the effects of the energy density (Eq. (43)). This may be seen more clearly by using the Einstein's equations with the tensor of Eq. (44) to find the metric around a wiggly string. The result in the weak field limit (small  $G\mu$ ) is[77]

$$ds^{2} = (1 + h_{00})(dt^{2} - dz^{2} - (1 - 4G\mu_{eff})^{2}r^{2}d\varphi^{2})$$
(45)

with

$$h_{00} = 4G(\mu_{eff} - T)ln(r/r_0) \tag{46}$$

where  $r_0$  is an integration constant. Clearly, in the presence of wiggles  $(\mu_{eff} \neq T)$  the Newtonian potential  $h_{00}$  is non-zero. The change of the azimouthal variable  $\varphi$  to the new variable  $\varphi' \equiv (1 - 4G\mu_{eff})\varphi$  makes the metric (45) very similar to the Minkowski metric with the crucial difference of the presence of the Newtonian  $h_{00}$  term and the fact that the new azimouthal variable  $\varphi'$  does not vary between 0 and  $2\pi$  but between 0 and  $2\pi - 8\pi G\mu_{eff}$ . Therefore there is a deficit angle[81]  $\alpha = 8\pi G\mu_{eff}$  in the space around a wiggly or non-wiggly string. Such a spacetime is called conical (Fig. 8) and leads to several interesting cosmological effects especially for moving long strings.

Figure 8: The gravitational effects of a long string: The string deficit angle  $\alpha$  leads to sharp discontinuities in the temperature of the CMB, velocity fluctuations in matter and formation of wakes, and lensing of galaxies and quasars. The Doppler and Sachs-Wolfe effects (see section 6.2) due to plasma velocities and potential fluctuations on the last scattering surface  $(t_{rec})$  are also illustrated.

#### 4.2 Velocity Fluctuations

The main mechanism by which strings create perturbations that could lead to large scale structure formation is based on velocity perturbations created by moving long strings. Long, approximately straight strings moving with velocity  $v_s$  induce velocity perturbations to the surrounding matter directed towards the surface swept in space by the string. This effect may be seen more clearly by using cartesian coordinates[77].

Consider a straight long straight long string moving on the y-z plane with velocity  $v_s$  (Fig. 8). By transforming the line element of Eq. (45) to 'shifted' cartesian coordinates defined as

$$y' \equiv r \sin \varphi' \simeq y - r \cos \varphi \, 4G \mu_{eff} \varphi \tag{47}$$

$$x' \equiv r \cos \varphi' \simeq r \cos \varphi = x \tag{48}$$

we obtain

$$ds^{2} = (1 + h_{00})(dt^{2} - dz^{2} - dx^{2} - dy'^{2})$$
(49)

where  $y' \equiv y - 4G\mu_{eff}\varphi x$ . The geodesic equations for a test particle in the cosmic string spacetime are of the form

$$2\ddot{x} = -(1 - \dot{x}^2 - \dot{y}^2)\partial_x h_{00} \tag{50}$$

$$2\ddot{y}' = -(1 - \dot{x}^2 - \dot{y}'^2)\partial_y h_{00} \tag{51}$$

Using the form of  $h_{00}$  from Eq. (46) and perturbing around the initial particle trajectory (on the string frame)

$$x = v_s t y' = y_0 = const (52)$$

the geodesic equations become

$$\ddot{x} = -\frac{1}{2}(1 - v_s^2)4G(\mu_{eff} - T)\frac{x}{r^2}$$
 (53)

$$\ddot{y}' = -\frac{1}{2}(1 - v_s^2)4G(\mu_{eff} - T)\frac{y'}{r^2}$$
(54)

A heuristic solution to these equations may be obtained as follows[77]: The Newtonian force induced by the wiggly string on a particle at distance r has a magnitude (cf Eq. (53-54))

$$F = \frac{2mG(\mu_{eff} - T)}{\gamma_s r} \tag{55}$$

and is effective for approximatelly

$$\Delta t \simeq \frac{r}{v_s} \tag{56}$$

Therefore the magnitude of the induced velocity will be approximatelly

$$\dot{y}' \simeq \frac{F}{m} \Delta t \simeq \frac{2G(\mu_{eff} - T)}{\gamma_s v_s}$$
 (57)

and by symmetry it is directed towards the surface swept by the string. The exact solution to the system of Eq. (53-54) turns out to be very similar

$$\dot{y}' \equiv \dot{y} - 4\pi G \mu_{eff} v_s \gamma_s \simeq \frac{2\pi G(\mu_{eff} - T)}{\gamma_s v_s} \tag{58}$$

and therefore the total velocity perturbation induced by a moving long string to surrounding matter close to the surface swept by the string is

$$\Delta v = \frac{2\pi G(\mu_{eff} - T)}{\gamma_s v_s} + 4\pi G \mu_{eff} v_s \gamma_s \tag{59}$$

where the first term is due to the Newtonian interaction of the string wiggles with matter while the second term is an outcome of the conical nature of the spacetime.

### 4.3 Microwave Background Fluctuations

Another particularly interesting effect of the string induced deficit angle is the creation of a characteristic signature on CMB photons. The type of this signature may be seen in a heuristic way as follows: Consider a straight long string moving with velocity  $v_s$  between the surface of last scattering occurring at  $t_{rec}$  and an observer at the present time  $t_0$  (Fig. 8). The metric around the string is approximated by Eq. (49) and at large distances from the string core we have

$$dy' \simeq dy - 4G\mu_{eff}\varphi dx = dy - 4G\mu_{eff}\varphi v_s \gamma_s dt \equiv dy - V(\varphi)dt$$
 (60)

For photons we have  $ds^2 = 0$  and therefore the Newtonian term  $h_{00}$  has no effect. Thus the presense of the moving long string between the observer

and the last scattering surface induces an effective Doppler shift to the CMB photons. For photons reaching the observer through the 'back' ('front') of the string we have

$$(\frac{\delta T}{T})_{1,(2)} = (\frac{\delta v}{v})_{1,(2)} = \pm (V(\varphi = 2\pi) - V(\varphi = \pi)) = \pm 4\pi G \mu_{eff} v_s \gamma_s$$
 (61)

where the 1(2) and +(-) refer to photons passing through the 'back' ('front') of the string.

Therefore a moving long string present between  $t_{rec}$  and today induces line step-like discontinuities on the CMB sky with magnitude [82, 83]

$$\frac{T_1 - T_2}{T} = 8\pi G \mu_{eff} v_s \gamma_s \tag{62}$$

Notice that there is no Newtonian term inversely proportional to the wiggly string velocity as was the case for the induced velocity perturbations. In section 6 it will be shown that Eq. (61) can be used to construct a superposition of long string perturbations thus constructing approximations to the predicted CMB maps.

# 4.4 Lensing

The existence of the deficit angle in the cosmic string space-time implies that strings act as gravitational lenses with certain characteristic properties[81, 83, 84]. A long string present between a quasar and an observer (Fig. 8) will lead to the formation of double quasar images for the observer. The separation angle of the two images depends on the magnitude of the deficit angle and may be found by simple geometrical considerations. Using Fig. 8 the separation angle  $\Delta\theta$  is obtained as

$$(l+d)\sin(\frac{\Delta\theta}{2}) = \sin(\frac{\alpha}{2}) \Rightarrow \Delta\theta \simeq 8\pi G \mu_{eff} \frac{l}{l+d} \stackrel{<}{\sim} 5$$
" (63)

Therefore a gravitational lensing event induced by a cosmic string is expected to involve a number of neighbouring double images with typical separation of a few arcsec. Such a candidate event has indeed been observed and it will be discussed in some detail in section 5.5.

#### 5 Structure Formation

#### 5.1 Sheets of Galaxies, Filaments

In the cosmic string model for structure formation, small and intermediate scale structure (galaxies and clusters) is seeded by string loops while large scale structure is produced by perturbations induced by long strings.

A loop with radius R has a mass  $M_l = \beta R \mu$  where  $\beta$  is a parameter approximatelly equal to  $2\pi$  and on distances much larger than its radius it produces a gravitational field which is identical to the field of a point mass with mass  $M_l[85]$ . Therefore string loops can act as seedlike perturbations leading to the formation of clusters and galaxies. Recent simulations[71, 72] however have shown that the typical size of loops is probably too small to have a significant effect on the formation of objects like galaxies or clusters. This implies that the simple 'one loop one object' assumption that was made in the early days of the cosmic string model is probably incorrect and more sophisticated methods must be developed to study the way small and intermediate structure forms in the string model.

The indicated relatively small importance of loops further amplifies the cosmological role of long strings. These strings can lead to large scale structure formation through the velocity perturbations, produced during their motion, to surrounding matter [86]. As discussed in section 4 long strings moving with velocity  $v_s$  produce velocity perturbations directed towards the surface they sweep in space. These perturbations whose initial magnitude is given by Eq. (59), grow gravitationally and within approximatelly a Hubble time t they form planar density perturbations called wakes [87, 86, 88, 89, 90] (Fig. 8). The gravitational growth of wakes can be calculated analytically in the linear regime using a simple but powerful method known as the the Zeldovich approximation. Using this method the thickness and typical dimensions of the dominant predicted planar structures can be calculated [89] and the result can be compared with observations of redshift surveys in order to test the cosmic string model. In what follows I will sketch the basic steps of the calculation involving the Zeldovich approximation.

Consider a long straight string moving with velocity  $v_s$  and sweeping a plane in an expanding universe. Consider also a test particle located a physical distance h(t) from the plane swept by the string. The scale h(t) will initially grow with the universe expansion but due to the string induced

velocity perturbation the growth will be decelerated by gravity, the scale h(t)will stop expanding, it will turn around and collapse on the string induced wake. In order for the planar structure formed to be able to fragment and lead to the formation of galaxies and clusters within it, it is necessary that the developed overdensity be nonlinear i.e.  $\frac{\delta \rho}{\rho} \gtrsim 0$ . It may be shown that this condition is indeed realized within the scales  $h_{nl}(t)$  that have turned around at a given time t. Thus, the scale  $h_{nl}(t)$  that turns around at t is called the nonlinear scale at time t and the time when a scale h turns around to collapse is called the time of non-linearity  $t_{nl}(h)$  for the scale h. Clearly,  $h_{nl}(t)$  defines the thickness of the planar structure at the time t. The length of this structure is approximated by the coherence length of the string which is given by the horizon scale t while its width is approximated by the distance  $v_s t$  travelled by the coherent portion of the string within an expansion time t.

Observations indicate that the typical thickness of the observed sheets of galaxies is about  $5h^{-1}Mpc$ . By demanding  $h_{nl}(t_0, G\mu) = 5h^{-1}Mpc$  i.e. that the predicted thickness of string induced sheets of galaxies is equal to the observed, the single free parameter of the model  $G\mu$  can be fixed. This normalization can then be compared with others coming from other observations and also from microphysical constraints. The length and width of the dominant structures can also be obtained.

In the context of the Zeldovich approximation the physical (Eulerian) coordinate  $\vec{r}$  of a test particle with initial comoving position  $\vec{q}$  (Lagrangian coordinate) is written as

$$\vec{r}(\vec{q},t) = a(t)(\vec{q} - \vec{\Psi}(\vec{q},t)) \tag{64}$$

where  $\vec{\Psi}$  is the comoving displacement induced by the initial perturbation. In order to find the comoving scale  $q_{nl}(t)$  that turns around at time t we must first use dynamics to find  $\vec{\Psi}$  and then solve  $\dot{\vec{r}} = 0$  to find  $q_{nl}(t)$ . This calculation is outlined below.

The dynamics of the Eulerian coordinate  $\vec{r}$  may be obtained in the Newtonian approximation using the equations

$$\ddot{\vec{r}}(\vec{q},t) = -\frac{\partial}{\partial \vec{r}} \Phi(\vec{r},t) \tag{65}$$

$$\ddot{\vec{r}}(\vec{q},t) = -\frac{\partial}{\partial \vec{r}} \Phi(\vec{r},t)$$

$$\frac{\partial^2}{\partial \vec{r}^2} \Phi(\vec{r},t) = 4\pi G \rho(\vec{r},t)$$
(65)

In addition, mass conservation implies that the mass in a Eulerian volume  $d^3r$  should be equal to the mass in the corresponding Lagrangian volume  $a^3d^3q$  *i.e.* 

$$\rho(\vec{r}, t)d^3r = a(t)^3 \rho_0(t)d^3q \tag{67}$$

or

$$\rho(\vec{r},t) = a(t)^3 \rho_0(t) \frac{1}{\det\left|\frac{d\vec{r}}{d\vec{q}}\right|} \simeq \rho_0(t) \left(1 + \frac{\partial}{\partial \vec{q}} \vec{\Psi}(\vec{q},t)\right)$$
(68)

From Eq. (66) and Eq. (68) we obtain to linear order in  $\vec{\Psi}$ :

$$\frac{\partial}{\partial \vec{r}} \Phi(\vec{r}, t) \simeq 4\pi G \left[ \frac{1}{3} \rho_0(t) \vec{r} + \rho_0(t) a(t) \vec{\Psi}(\vec{q}, t) \right]$$
 (69)

Using the Friedman equation Eq. (3) in Eq. (69) and using also Eq. (64-65) we obtain

$$\ddot{\vec{\Psi}} + 2\frac{\dot{a}}{a}\dot{\vec{\Psi}} + 3\frac{\ddot{a}}{a}\vec{\Psi} = 0 \tag{70}$$

which with the appropriate initial conditions can determine the evolution of  $\vec{\Psi}$ 

The initial conditions corresponding to the velocity perturbation induced by a moving long string at an initial time  $t_i$  are of the form

$$\vec{\Psi}(t_i) = 0 \tag{71}$$

$$\dot{\vec{\Psi}}_x(t_i) = \dot{\vec{\Psi}}_y(t_i) = 0 \tag{72}$$

$$\Delta v \equiv a(t_i)\dot{\vec{\Psi}}_x(t_i) = 4\pi G\mu v_s \gamma_s f \tag{73}$$

with  $f = 1 + \frac{1 - \frac{T}{\mu_{eff}}}{2(v_s \gamma_s)^2}$  as implied by Eq. (59).

The growing mode solution of Eq. (70) with initial conditions (71-73) in the matter era  $(a \sim t^{2/3})$  can easily be found to be of the form

$$\Psi(t) \simeq \frac{3}{5} \Delta v \left(\frac{t}{t_i}\right)^{2/3} \left(\frac{t_0}{t_i}\right)^{2/3} t_i \tag{74}$$

It is now straightforward to find the comoving scale  $q_{nl}(t)$  that becomes nonlinear and turns around at time t

$$\frac{d}{dt}(a(q_{nl} - \Psi(t))) = 0 \Rightarrow q_{nl}(t) = 2\Psi(t)$$
(75)

Using also the observational fact that  $q_{nl}(t_0) \gtrsim 5h^{-1}Mpc$  we may obtain a constraint on the only free parameter of the model

$$G\mu_{eff} \stackrel{>}{\sim} 0.7(v_s \gamma_s f)^{-1} \times 10^{-6}$$
 (76)

where  $t_i = t_{eq}$  has been used in Eq. (74) since fluctuations can not grow before  $t_{eq}$  due to pressure effects present in the radiation component. This result compares favourably with constraints coming from a completely different direction: microphysics. In order for GUTs to be consistent with low energy experiments and with constraints on baryon lifetime, the scale of GUT symmetry breaking  $\eta$  must be of the order  $10^{16}$ GeV. For strings formed during a GUT phase transition this implies that

$$(G\mu)_{GUT} \simeq (G\eta^2)_{GUT} \simeq 10^{-6} \tag{77}$$

which compares well with the corresponding constraint from macrophysics (Eq. (76)). This striking agreement, which was first observed in studies of galaxy formation by string loops[91], between constraints coming from completely different directions is an exciting example of a meeting point between cosmology and particle physics and has also been one of the most attractive features of the cosmic string model.

The earliest string wakes forming at  $t_{eq}$  are the most numerous and also they have the longest time to grow. Therefore they give rise to the dominant sheetlike structures by today. Their typical dimensions are determined by the size of the comoving horizon at  $t_{eq}$  and by the nonlinear scale  $q_{nl}(t_{eq}, t_0)$  which determines their present thickness (Eq. (75)). Thus the predicted dimensions of these structures are

$$\xi t_{eq}^{com} \times v_s t_{eq}^{com} \times q_{nl}(t_{eq}, t_0) \simeq \xi 40 \times v_s 40 \times 5Mpc^3$$
 (78)

where  $\xi \lesssim 1$  is the coherence length of long strings. The above predicted dimensions compare reasonably well with observations assuming relativistic strings. Simulations have shown that a large portion of long strings have relatively small velocities  $v_s \simeq 0.15$  on horizon scales. Such strings will tend to form structures that are more filamentary than sheetlike.

The above discussion on the form and dimensions of the predicted large scale structure has not taken into account the effects of free streaming and therefore it is valid only for CDM. The effects of free streaming present in the case of HDM can be taken into account by preventing the growth of scales smaller than the comoving free streaming scale

$$\lambda_j^{com} = v_{\nu}(t)t/a(t) \tag{79}$$

where the velocity  $v_{\nu}$  of HDM particles (eg neutrinos) starts droping like 1/a(t) after  $T \simeq m_{\nu}$  when they become nonrelativistic. A sketch of the time dependence of  $\lambda_j^{com}$  is shown in Fig. 9.

Figure 9: The time dependence of the free streaming scale  $\lambda_j^{com}$ .

An important value for  $\lambda_j$  is its maximum value  $\lambda_j^{max}$  which for adiabatic fluctuations produced during inflation determines the minimum scale that can form independent of larger scales (without fragmentation). Adiabatic (but not seedlike) perturbations on all scales smaller than  $\lambda_j^{max}$  are erased by free streaming and structures on these scales can only form by fragmentation of larger objects. This is a problem in adiabatic perturbations with HDM because observations indicate[92] that galactic and cluster scales formed earlier than larger scales. This is difficult to explain in models where fragmentation is the only mechanism to form smaller scale structures. Seeds like cosmic strings survive free streaming and therefore smaller scale fluctuations in models with seeds + HDM are not erased but their growth is only delayed by free streaming[93, 94]. Thus galaxies and clusters can in principle form independently of large scale structure in these models. For a neutrino with mass  $m_{\nu} = 25eV$  (enough to produce  $\Omega = 1$  for h = 1/2) we find

$$\lambda_i^{max} \simeq \lambda_i(t_{eq}) \simeq 6h_{50}^{-2}Mpc$$
 (80)

and therefore the growth of all scales less than  $6h_{50}^{-2}Mpc$  is delayed by free streaming. Thus the introduction of HDM in the string model has two main effects. First it delays the growth of smaller scales thus transferring more power on large scales and second the delayed growth tends to increase the required value of  $G\mu$  for nonlinear structures to form by today. A detailed calculation shows[89] that

$$(G\mu)_{HDM} \simeq 2 \times 10^{-6} > (G\mu)_{CDM}$$
 (81)

#### 5.2 Peculiar Velocities

Using the result of Eq. (74) for the comoving displacement  $\Psi$  it is straightforward to find the magnitude and coherence length of peculiar velocities  $u(t_0, t_i)$  produced by long strings at an initial time  $t_i$  as observed at the present time  $t_0$ . The typical magnitude of these velocities is[95]

$$u(t_0, t_i) = \dot{\Psi}(t_0, t_i) = \frac{2}{5} \Delta v(\frac{t_0}{t_i})^{1/3} \qquad (t_i \ge t_{eq})$$
 (82)

where  $\Delta v \equiv 4\pi G \mu_{eff} v_s \gamma_s f$ . The coherence length of these velocity fields is given by the coherence length of the long string that produced them which in turn is about equal to the comoving horizon scale  $L(t_i) \equiv t_i^{com} = \int_{t_i} \frac{dt}{a(t)} \sim t_i^{1/3}$ . Thus the magnitude of the predicted velocity field with coherence scale L is

$$u(t_0, L) \simeq 300\mu_6 h \frac{L_{eq}}{L} km/sec \tag{83}$$

where  $\mu_6 \equiv G\mu/10^{-6}$ ,  $L_{eq} \equiv t_{eq}^{com} = 14h^{-2}Mpc$ . This result is not in good agreement with peculiar velocity observations on large scales which indicate the presence of velocity fields with magnitude of about 600km/sec coherent on all scales from  $10h^{-1}Mpc$  to larger than  $50h^{-1}Mpc$ . Even though it is possible to play with the normalization of the model to induce agreement with observations on a particular scale, the  $L^{-1}$  scaling does not allow agreement on a large range of scales. This problem of the cosmic string model which also appears in the standard adiabatic CDM model can be addressed by assuming velocity bias which essentially means that the observed velocity fields do not represent accurately the underlying velocity fields of dark matter since luminous matter evolves differently than dark matter. The motivation for such a conjecture however is not particularly appealing especially on these large scales.

### 5.3 Power Spectrum

An important quantity that characterizes a pattern of fluctuations  $\frac{\delta \rho}{\rho}(\vec{x})$  is the *power spectrum*. Consider a Fourier expansion of a fluctuation pattern

$$\frac{\delta\rho}{\rho}(\vec{x}) = \int d^3k \frac{\delta\rho}{\rho}(\vec{k})e^{i\vec{k}\vec{x}} \tag{84}$$

The power spectrum  $P(\vec{k})$  of the pattern is then defined as the ensemble average

$$P(\vec{k}) \equiv <|\frac{\delta\rho}{\rho}(\vec{k})|^2 > \tag{85}$$

It may be shown that the correlation function  $C(\vec{x})$  of the pattern smoothed on a scale  $l_0 \sim k_0^{-1}$  can be obtained as the Fourier transform of the power spectrum *i.e.* 

$$C(\vec{x}) \equiv \langle \frac{\delta \rho}{\rho} (\vec{x}_1) \frac{\delta \rho}{\rho} (\vec{x}_1 + \vec{x}) \rangle_{x_1} = \int d^3k P(\vec{k}) e^{i\vec{k}\cdot\vec{x}} W(k - k_0)$$
 (86)

where  $W(k-k_0)$  is a filter function which filters out the scales that do not contribute due to smoothing and finite volume effects. Thus, the contribution of scales smaller than  $l_0 \sim k_0^{-1}$  to the variance of the fluctuations is approximated by

$$<(\frac{\delta\rho}{\rho}(\vec{x}))^2>_{l_0}=C(0)_{k_0}\equiv\delta(k_0,t)^2\simeq k_0^3P(k_0)$$
 (87)

Now the existence of the scaling solution implies that string induced perturbations  $\delta_s$  have a fixed magnitude on horizon scales at any given time. Thus

$$\delta_s(\lambda_k = t, t) = constant$$
 (88)

where  $\lambda_k = a(t) \frac{2\pi}{k}$  is the physical smoothing scale. At a later time t in the matter era the fluctuations will have grown to

$$\delta(k,t) = \left(\frac{t}{t_i}\right)^{2/3} \delta(\lambda_k = t_i, t_i) \tag{89}$$

But

$$t_i = \lambda_k \sim a(t_i)/k \sim t_i^{2/3}/k \Rightarrow t_i \sim k^{-3}$$
(90)

and therefore combining Eq. (88) and Eq. (89) we obtain  $\delta(k,t) \sim k^2$  which combined with Eq. (87) gives

$$P(k) \sim k \tag{91}$$

known as the scale invariant[96] Harisson-Zeldovich power spectrum. This is a generic type of spectrum which is also predicted by models based on inflation[97]. Any large variation from the scale invariant spectrum is cosmologically unacceptable since it would lead to ultraviolet or infrared disasters in the magnitude of fluctuations.

**Figure 10:** The *log* of the power spectrum vs the *log* of the scale for strings (dashed) and gaussian scale invariant fluctuations. In each case the curve with more power on small scales corresponds to CDM, the other to HDM. (From Ref. [99]).

Given that growth of fluctuations starts at  $t_{eq}$ , perturbations on scales larger than the horizon at  $t_{eq}$  enter the horizon after  $t_{eq}$  and they keep growing without delay thus keeping their power law form  $P(k) \sim k$ . On the other hand fluctuations on smaller scales enter the horizon at earlier times and their growth is delayed until  $t_{eq}$  when matter dominates. The delay is larger the earlier the scale enters the horizon *i.e.* is larger for smaller scales. Thus, we expect a bending of the spectrum at smaller scales[98] to a power low  $P(k) \sim k^n$  with n < 1. An additional bending is expected to occur in the

case of HDM[99] due to the effects of free streaming which delay (erase) seed (adiabatic) fluctuations on small scales. In fact in the case of adiabatic fluctuations we have not only a bending but a *cutoff* of the spectrum at the maximum free streaming scale. The above discussion is illustrated in Fig. 10 where the spectra of adiabatic and string perturbations are plotted for CDM and HDM models. The attractive feature of the model of strings with HDM is the transfer of power to large scales without completely erasing the power on small scales. This is in agreement with observations showing more power on large scales than predicted by the standard adiabatic+CDM model and also allows for the independent growth and formation of structures on smaller scales. Detailed N-body simulations of the string+HDM model attempting to explore in more detail these features are currently in progress.

#### 5.4 Gravitational Radiation

A particularly interesting cosmological constraint that can be imposed on the cosmic string model is based on the gravitational radiation produced by oscillating massive loops[100, 101]. These oscillations are expected to lead to a stochastic gravitational wave background which could be detectable as perturbations of the period of msec pulsars[102]. The phase  $\varphi(t)$  of the periodic signal detected by a msec pulsar can be expanded as

$$\varphi(t) = \varphi_0 + \dot{\varphi}t - \frac{1}{2}\ddot{\varphi}t^2 + \varphi_R(t)$$
(92)

the first three terms can be modeled based on observations and pulsar physics while  $\varphi_R(t)$  is called the residual phase and is due to perturbations of the signal period induced by either gravitational waves or by other sources (pulsar intrinsic noise etc.). The quantity that characterizes the energy density of gravitational waves of angular frequency  $\omega$  is

$$\Omega_g(\omega) \equiv \frac{\omega \rho_g(\omega)}{\rho_0} \tag{93}$$

where  $\rho_g$  is the energy density in gravity waves. For the stochastic background produced by string loops it may be shown that

$$\Omega_g(\omega, G\mu) = 2.5 \times 10^{-8} \mu_6 \left(\frac{P}{2\pi}\right)^2 < \varphi_R^2(T) > h^{-4} \left(\frac{2\pi}{T}\right)^4$$
(94)

where

$$\langle \varphi_R^2(T) \rangle \equiv \langle \frac{1}{T} \int_t^{t+T} \varphi_R^2 dt \rangle$$
 (95)

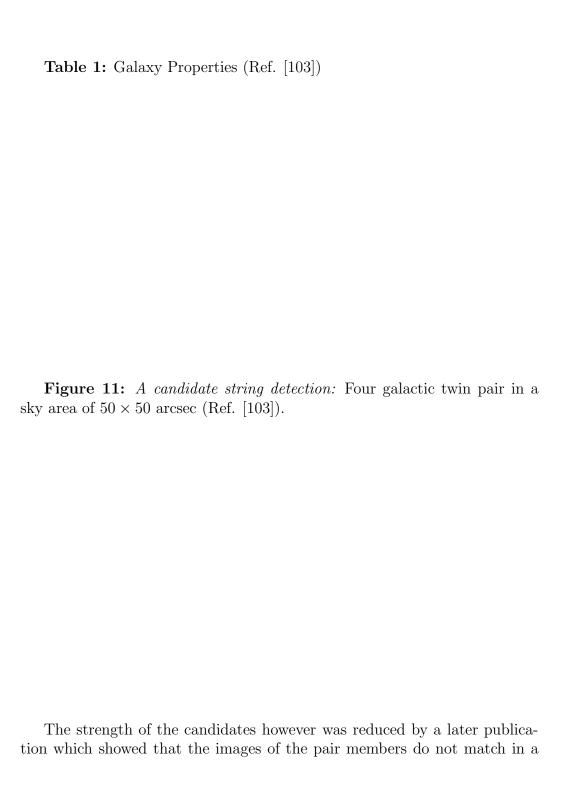
and P is the period of the signal in sec. The presently observed time residual is  $P < \varphi_R^2 > /2\pi \simeq 1.5 \mu sec$  and this implies an upper bound for  $\mu_6$  whose precise value depends on the string simulations. The most recent careful study of constraints from the msec pulsar[101] gives a bound on  $\mu_6$  of  $\mu_6 \lesssim 2 \times 10^{-6} h^{-8/3}$ . This result is based on the numerical simulations of Allen and Shellard[72] and it is projected that if the residual timing noise remains constant the bound in 1998 will be  $\mu_6 \lesssim 5 \times 10^{-8} h^{-8/3}$  thus effectively ruling out the model.

### 5.5 A String Detection?

The detection of cosmic string segments through the detection of multiple lensing pairs of galaxies or quasars is a very exciting prospect. The expected properties of such lensing events can be summarized as follows

- A number of  $N \gtrsim 3$  of galactic or quasar twin pairs is expected concentrated in a small region in the sky  $(eq 50'' \times 50'')$
- The angular separation of pairs is expected to be approximately constant of O(1'') as shown in Eq. (63).
- In contrast to most typical lensing events strings are expected to induce no magnification of the images during lensing due to the conical nature of their metric.
- The members of the lensed pair are expected to have very similar properties (redshifts, spectra *etc.*) since they originate from the same object.
- The redshift of the pair is expected to be relatively large to increase the probability for a string being present along the line of sight  $(z \gtrsim 0.1)$ .

An event that effectively fulfills all the above properties was detected in 1987[103] by Cowie and Hu who detected 4 twin pairs of galaxies in a  $50'' \times 50''$  angular region in the sky with typical angular separation 3", no magnification and very similar properties. These properties are shown in Table 1 (from Ref. [103]) while a contour plot of the twin pairs is shown in Fig. 11.



satisfactory way when images are studied in radio band[104]. Even though the issue is far from being resolved there is currently no clear evidence that these events are induced by a string lensing.

# 6 Cosmic Strings and the Microwave Background

### 6.1 Angular Spectrum Basics

A pattern of CMB temperature fluctuations is characterized by two classes of properties: properties of the angular power spectrum and statistical properties (probability distribution function etc.). I will give an introduction of the angular spectrum basics[105] and discuss the relevant predictions of the cosmic string model obtained by using a simple analytical approximation[106, 107]. The predicted statistical properties of the CMB fluctuations will be discussed also.

Consider a photon scattered for last time on the last scattering surface at  $t_{rec}$  and reaching an observer with observational resolution  $\Theta$  at time  $t_0$ . One of the main sources of CMB fluctuations is the Sachs-Wolfe effect which is the result of gravitational potential fluctuations on the last scattering surface. Thus, an initially isotropic photon wavefront has to climb out of a potential  $\delta\Psi$  whose depth varies with direction. The resulting fluctuations  $(\frac{\delta T}{T})_{\lambda}$ , smoothed on a scale  $\lambda$  on the last scattering surface are

$$\left(\frac{\delta T}{T}\right)_{\lambda} \sim \delta \Psi_{\lambda} \tag{96}$$

The gravitational potential due to a mass overdensity  $\delta \rho$  on a scale  $\lambda$  is

$$\delta\Psi_{\lambda} \sim \frac{G\delta M}{\lambda} \sim G\delta\rho_{\lambda}\lambda^2 \sim G\lambda^{(3+n)/2}\lambda^2 \sim \lambda^{(1-n)/2}$$
 (97)

where use was made of  $\delta \rho_{\lambda} \sim (k^3 P(k))^{1/2} \sim k^{(3+n)/2} \sim \lambda^{-(3+n)/2}$ . Now, Eq. (96) and Eq. (97) imply that

$$(\frac{\delta T}{T})_{\Theta} \sim \delta \Phi_{\Theta} \sim \Theta^{(1-n)/2}$$
 (98)

and therefore the correlation function at zero lag ( $\Delta\theta = 0$ ) for angular resolution  $\Theta$  is

$$C(\Delta\theta = 0)_{\Theta} \equiv \langle (\frac{\delta T}{T})^2 \rangle = (\frac{\delta T}{T})_{rms}^2 \sim \Theta^{(1-n)}$$
 (99)

where <> denotes ensemble average (equivalent to angular averaging with the ergodic hypothesis). Therefore for a scale invariant power spectrum (n = 1),  $(\frac{\delta T}{T})_{rms}$  is independent of the angular resolution

$$(\frac{\delta T}{T})_{rms} \sim constant$$
 (100)

Note that even for scale invariant primordial spectra (100) will be violated on angular scales less than the angular scale of the horizon at recombination  $(\Theta_{rec} \simeq z_{rec}^{-1/2} \simeq 0.03 rad \simeq 2^{0})$  due to microphysical processes taking place on subhorizon scales (Doppler effect *etc.*). Such processes are discussed below.

CMB fluctuations are usually measured on large parts of the sky and in some cases over the whole celestial sphere. Therefore a convenient basis to analyse these perturbations is not the Fourier basis but the *spherical harmonics*. A fluctuation pattern  $\frac{\delta T}{T}(\hat{q})$  can be expanded as

$$\frac{\delta T}{T}(\hat{q}) = \sum_{l,m} a_l^m Y_l^m(\theta, \phi) \tag{101}$$

Using the addition theorem, the lack of preferred direction and defining  $C_l \equiv <|a_l^m|^2>$  we may expand the angular correlation function  $C(\theta)$  using the angular spectrum coefficients  $C_l$ 

$$C(\theta) \equiv \langle \frac{\delta T}{T}(\hat{q}_1) \frac{\delta T}{T}(\hat{q}_2) \rangle = \frac{1}{4\pi} \sum_{l=0}^{\infty} (2l+1) C_l P_l(\cos \theta)$$
 (102)

where  $\cos \theta \equiv \hat{q}_1 \cdot \hat{q}_2$ . For observational experiments taking place on a relatively small part of the sky the contribution of low values of l is filtered out and the above expression reduces as expected to a two dimensional Fourier transform with the angular spectrum  $C_l$  playing the role of the power spectrum P(k)

$$C(\theta) = \frac{1}{4\pi} \sum_{l>1}^{\infty} (2l+1)C_l P_l(\cos\theta) \simeq \frac{1}{2\pi} \sum_{l>1} lC_l J_0(l\theta) \Rightarrow (103)$$

$$C(\theta)_{\Theta_0} \simeq \frac{1}{(2\pi)^2} \int d^2l C_l e^{i\vec{l}\cdot\vec{\theta}} W(l-l_0)$$
(104)

where  $W(l - l_0)$  is a filter function centered on the maximum sensitivity mode  $l_0$  and filtering out modes that are undetectable due to either limited sky coverage or limited resolution.

Consider the power law ansatz  $C_l \sim l^{\alpha}$ . The angular scale corresponding to the mode l may be approximated by  $\Theta_l = \frac{\pi}{l}$ . Therefore, using Eq. (104) we can express  $(\frac{\delta T}{T})_{rms}$  in terms of the resolution  $\Theta_0$  and comparing with Eq. (99) we can express  $\alpha$  in terms of the power spectrum index n *i.e.* 

$$C(0)_{\Theta_0} = (\frac{\delta T}{T})_{rms}^2 \sim l_0^2 C_{l_0} \sim \Theta_0^{-\alpha - 2}$$
 (105)

Now comparing Eq. (99) with Eq. (105) we obtain  $\alpha = n - 3$  and therefore

$$C_l \sim l^{n-3} \tag{106}$$

which is approximately valid for l > 1. Fig. 12 (from Ref. [115]) shows the form of the angular spectrum  $l^2C_l$  as predicted by some models based on adiabatic fluctuations.

Figure 12: The CMB angular spectrum as predicted by some typical models based on gaussian scale invariant fluctuations. Using appropriate filter functions for each experiment the predicted  $(\frac{\delta T}{T})_{rms}$  can be obtained.

Notice the flatness of the spectrum  $(l^2C_l = const)$  on angular scales less than the horizon at recombination  $(l \sim 100)$  which indicates the presence

of scale invariance. COBE, with angular resolution  $\Theta_0 \simeq 10^0$  and all sky coverage is sensitive to  $l \lesssim 35$  and therefore the COBE data can provide both the normalization and the primordial spectral index n. Even though the different ways to perform the analysis of the data lead to slight variations in the value of n = 1, the data are consistent with a scale invariant spectrum n = 1 and seem to favor a small positive tilt (blue spectrum, n > 1) over a negative tilt (red spectrum n < 1). Most models based on inflation tend to favor a small negative tilt of the spectrum[108].

Several experiments collect temperature data along one dimension in the sky for example along a meridian. The power spectrum index can also be derived by using the data from such one dimensional experiments. In order to avoid confusion with the two dimensional angular spectrum  $C_l$ , I will denote the one dimensional angular power spectrum by P(k) and the variable conjugate to the angle along the geodesic circle under consideration by k. This should not be confused with the density spectrum where a similar notation is usually used. The correlation function for a one dimensional pattern is the Fourier transform of P(k)

$$C^{1d}(\Delta\theta) \simeq \frac{1}{2\pi} \sum_{k} P(k)e^{ik\Delta\theta}W(k-k_0)$$
 (107)

where  $W(k - k_0)$  is a filter function corresponding to the resolution of the experiment. By isotropy  $C^{1d}(\Delta\theta) = C^{2d}(\Delta\theta)$  and also  $k \simeq l$  since they are both conjugate of the angular scale  $\Delta\theta$ . Therefore from Eq. (104) and Eq. (107) we obtain

$$l^2C_l \simeq kP(k) \sim k^{n-1}, \qquad (\frac{\delta T}{T})_{rms} = C^{1d}(0) = C^{2d}(0)$$
 (108)

These results will be applied in approximating the predicted angular power spectrum of the string model.

### 6.2 String Angular Spectrum

There are three main sources that can lead to CMB temperature fluctuations in the context of the cosmic string model:

• Kaiser-Stebbins[82, 83] perturbations due to moving long strings present between  $t_{rec}$  and the present.

- Potential fluctuations on the last scattering surface (Sachs-Wolfe effect[109]) induced by long string wakes and loops with their gravitationally accreted matter.
- Doppler perturbations induced by the local peculiar velocities of the plasma on which photons scatter for last time (see eg Ref. [110]).

The above three types of perturbations are shown schematically in Fig. 8. Therefore the total string induced CMB temperature fluctuation may be written as

 $\left(\frac{\delta T}{T}\right)_{tot} = \left(\frac{\delta T}{T}\right)_{KS} + \left(\frac{\delta T}{T}\right)_{SW} + \left(\frac{\delta T}{T}\right)_{D} \tag{109}$ 

Each one of these three contributions involves the superposition of some type of seeds and therefore in order to calculate it we must address the following two questions

- 1. How can seeds be superposed?
- 2. What type of seed should be superposed in each case?

I will here briefly address the first question. A detailed study of both questions may be found in Ref. [111]. For simplicity I will focus on one dimensional data. Consider a geodesic circle in the sky and a seed CMB temperature fluctuation function  $f_1(\theta)$  with amplitude  $a_1$  and angular scale  $\Psi$  (Fig. 13) centered at a random angular position  $\theta_1$ .

**Figure 13:** Superposition of a seed on a geodesic circle on the sky.

A random superposition of N such seed functions will lead to a temperature pattern of the form

$$f(\theta) = \sum_{n=1}^{N} a_n f_1^{\Psi}(\theta - \theta_n) = \sum_{n=1}^{N} a_n \frac{1}{2\pi} \sum_{k=-\infty}^{+\infty} \tilde{f}_1^{\Psi}(k) e^{ik(\theta - \theta_n)}$$
(110)

and therefore the Fourier transform  $\tilde{f}(k)$  of the pattern may be written as

$$\tilde{f}(k) = \tilde{f}_1^{\Psi}(k) \sum_{n=1}^{N} a_n e^{ik\theta_n}$$
(111)

Thus, the power spectrum corresponding to the pattern is

$$P_0(k) = \langle |\tilde{f}(k)|^2 \rangle = N \langle |a_n|^2 \rangle |\tilde{f}_1^{\Psi}(k)|^2$$
 (112)

In realistic cases however when the seed perturbations are induced by topological defects, the size  $\Psi$  of the seed function will not be fixed but will grow as the horizon scale (the characteristic coherence scale of scaling defects) grows. Thus defect perturbations produced at later times when the horizon scale is larger will have a larger characteristic angular scale in the sky. Assume for example that the comoving horizon grows by a scale factor  $\alpha$  i.e.  $t^{com} \to \alpha t^{com}$ . This implies that the angular scale of the horizon  $\Theta_h$  and the seed size  $\Psi$  will grow by the same factor while the total number of seeds N superposed along a circle at this later time will be smaller by the same factor

$$\Theta_h \to \alpha \Theta_h \Rightarrow (\Psi \to \alpha \Psi, \quad N \to N/\alpha)$$
 (113)

The power spectrum  $P_Q(k)$  corresponding to the resulting pattern after Q such expansion steps may be written as

$$P_Q(k) = \sum_{q=0}^{Q} \frac{N}{\alpha^q} |f_1^{\alpha^q \Psi}(k)|^2 < |a_n|^2 >$$
 (114)

where the total number of steps Q may be obtained from the ratio of the maximum over minimum seed (or horizon) size while the total number of seeds at the first expansion step is the number of defects per horizon scale (obtained from the simulations leading to the scaling solution) times the total number of horizons present on the circle during the first expansion step

$$\Psi_{max} = \alpha^Q \Psi_{min} \qquad N = M \frac{2\pi}{\Theta_{min}}$$
 (115)

Eq. (114) may now be used to find the contribution to the total spectrum from each one of the following perturbation types

- Kaiser-Stebbins (KS) perturbations
- Potential perturbations due to wakes (W) and loops (L) with their accreted matter present on the last scattering surface.
- Doppler (D) perturbations due to plasma velocities induced by strings (photons scattered on moving plasma suffer Doppler shift).

The quantities that need to be specified in Eq. (114) for each one of the above perturbation types are, the type of seed function  $f_1$ , the number of seeds per horizon M and the range of seed scales that need to be superposed. Assuming independent contributions from each perturbation type, the total spectrum  $P_{tot}$  may be obtained as a sum of the partial spectra as

$$P_{tot}(k) = P_{KS}(k) + P_W(k) + P_L(k) + P_D(k)$$
(116)

The detailed derivation of the form of  $P_{tot}$  may be found in Ref. [111]. There it is shown that  $P_{tot}(k)$  depends on four parameters; the single free parameter of the cosmic string model  $G\mu$  which may be normalized by comparing with the CMB COBE data or by large scale structure observations and three other parameters which may in principle be fixed by comparing with numerical simulations. These parameters are defined as

$$b \equiv M < (v_s \gamma_s)^2 > \tag{117}$$

$$f \equiv 1 + \frac{1 - T/\mu_{eff}}{2(v_s \gamma_s)^2} \tag{118}$$

$$\xi \quad : \quad \Psi = \xi \Theta_h(t)/2 \tag{119}$$

where  $\xi$  is the string curvature radius  $\Psi$  as a fraction of the horizon scale  $\Theta_h(t)$  and f determines the wiggliness of long strings as defined previously. These three parameters may be fixed either by comparing directly with string simulations or by comparing the CMB spectral contribution  $P_{KS}(k)$  of Eq. (116) with the corresponding spectrum derived by propagating a photon wavefront through a simulated string network[112, 113]<sup>6</sup>. Both of these approaches have been pursued in Ref. [111] with results that are consistent with each other.

 $<sup>^6</sup>P_{tot}$  can not be used because CMB simulations with strings have not included so far the effects of potential and Doppler fluctuations

**Figure 14:** The total spectrum (a) including Kaiser-Stebbins, Sachs-Wolfe and Doppler fluctuations obtained as discussed in the text. The contribution of each individual component is also shown (b) (Ref. [111]).

The total spectrum  $P_{tot}(k)$  in units of  $(G\mu)^2$ , obtained after the above normalization, is shown in Fig. 14a while the contribution of each type of perturbation is shown in Fig. 14b

Doppler CMB fluctuations are due mainly to long strings present on the last scattering surface and therefore their characteristic scale corresponds to the coherence scale of those strings. By the scaling solution, this scale is of the order of the horizon at  $t_{rec}$  ( $\Theta_h(t_{rec}) \simeq 2^0 \Rightarrow k_h(t_{rec}) \simeq 100$ ). This explains the existence of a well defined peak for the Doppler term. The fact that the magnitude of this peak is significantly larger than the magnitude of the scale invariant Kaiser-Stebbins (KS) term may be understood as follows: The magnitude of the contribution to the KS term by each long string is

$$\left(\frac{\delta T}{T}\right)_{KS} = 4\pi G \mu v_s \gamma_s \hat{k} \cdot (\hat{v}_s \times \hat{s}) \tag{120}$$

where  $\hat{k}$  is the unit photon wave-vector and  $\hat{s}$  is the unit vector along the string. The corresponding contribution to the Doppler term is

$$(\frac{\delta T}{T})_D = \hat{k} \cdot \delta \vec{v} = 4\pi G \mu v_s \gamma_s \hat{k} \cdot (\hat{v}_s \times \hat{s}) f = (\frac{\delta T}{T})_{KS} f$$
 (121)

where  $f \simeq 6$  (f defined in Eq. (118)) according to simulations[71]. Thus we expect the Doppler term to dominate over the KS term for  $k \simeq k_h(t_{rec}) \simeq 100$  as is in fact seen in Fig. 14b The negligible contribution of loops (dotted line in Fig. 14b) to the total spectrum may also be understood by considering the fact that the typical loop radius is a tiny fraction (about  $10^{-4}$ ) of the horizon as shown by simulations. Therefore a typical loop present on the last scattering surface at  $t_{rec}$  corresponds to an angular scale of about 0.3 arcsec which is way above the resolution of any present experiment.

It is now easy to normalize the remaining parameter  $G\mu_{eff}$  by using the COBE DMR data. The angular correlation function predicted for the COBE (DMR) experiment can be expressed in terms of  $P_{tot}(k)$  and the window function  $W(k-k_0) \simeq e^{-\frac{k^2}{(2\cdot 18)^2}}$  as shown in Eq. (107). By demanding agreement with the detected  $(\frac{\delta T}{T})_{rms}$  we have

$$\left(\frac{\delta T}{T}\right)_{rms}^{DMR} = (C(0))^{1/2} = 1.1 \times 10^{-6} \Rightarrow (G\mu)_{eff} = 1.6 \times 10^{-6}$$
 (122)

Figure 15: The cosmic string predicted correlation function smoothed on COBE scales. Superimposed are the first year COBE data (Ref. [111]).

This result is consistent with previous analytical studies[106] and with numerical simulation studies[112, 113]. Fig. 15 shows  $C(\theta)$  obtained by Eq. (107) (normalized with Eq. (122)) superposed with the COBE data. As

expected by the scale invariant nature of the string perturbations on COBE scales, the agreement is fairly good.

The predicted power spectrum index can be found with a best fit based on Eq. (108). By using modes with  $k \leq 20$  and the spectrum of Fig. 14a we find

$$n \stackrel{>}{\sim} 1.35 \pm 0.5 \tag{123}$$

Eq. (123) is a lower limit to the actually predicted n because Eq. (114) gives a slight overestimation of power on large scales<sup>7</sup> by assuming  $\alpha$  fixed at all expansion steps (the expression  $\Theta_h(t) \simeq z(t)^{-1/2}$  was used for all redshifts z(t) even though this approximation starts breaking down at low redshifts).

**Table 2**:Detections of  $\frac{\Delta T}{T_{rms}} \times 10^6$  and the corresponding predictions of the string ( $\Omega_0 = 1$ , h = 0.5, no reionization,  $\Lambda = 0$ ) and inflationary models ( $0.8 \le n \le 1.0$ ,  $\Lambda = 0$ ) normalized on COBE.

Experiment	$k_0$	$\Delta k$	Detection	Strings	Inflation
COBE	0	18	$11 \pm 2$	$11 \pm 3$	$11 \pm 2$
TEN	20	16	$\leq 17$	$13 \pm 3$	$9 \pm 1$
SP91	80	70	$11 \pm 5$	$20 \pm 5$	$12 \pm 2$
SK	85	60	$14 \pm 5$	$19 \pm 4$	$12 \pm 3$
MAX	180	130	$\leq 30 \; (\mu Peg)$	$21 \pm 5.5$	$16 \pm 5$
MAX	180	130	$49 \pm 8 \; (GUM)$	$21 \pm 5.5$	$16 \pm 5$
MSAM	300	200	$16 \pm 4$	$19 \pm 4$	$24 \pm 6$
OVRO22	600	350	-	$13 \pm 4$	$17 \pm 7$
WD	550	400	$\leq 12$	$17.5 \pm 4.5$	$7 \pm 2$
OVRO	2000	1400	$\leq 24$	$13.5 \pm 3.5$	$7\pm3$

If the exact  $\Theta_h(z)$  relation was used,  $\alpha$  would need to be larger at late times thus reducing the number of expansion steps at large scales. The result would be a slightly reduced power on large scales and a tilt of the spectrum towards n > 1 for the scale invariant KS contribution. This effect was taken into account in Ref. [112] where it was shown that it can increase the KS contribution to n by about 40%. Here, the effect on the total spectrum will be smaller since the other contributions remain unaffected by this. Using  $W(k) = e^{-(k-k_0)^2/\Delta k^2}$  and fixing  $k_0$ ,  $\Delta k$  for some of the ongoing experiments we are in position to predict the corresponding value of  $\frac{\Delta T}{T_{rms}}$  thus testing the cosmic string model. These predictions with  $1\sigma$  errors coming from the

<sup>&</sup>lt;sup>7</sup>I thank Neil Turok for pointing this out

variance of  $a_n^2$  are shown in Table 2. I also show some of the detections and upper limits existing to date[114] as well as the predictions of inflationary models for  $0.8 \le n \le 1.0$ ,  $\Lambda = 0$  [115]). At this time both inflationary models and cosmic strings appear to be consistent with detections at the  $1\sigma$  level. However, as the quality of observations improves, this may very well change in the near future.

### 6.3 Statistical Tests

The predictions of the string model on the CMB angular spectrum are useful in testing the model by comparing the amplitude of the predicted CMB fluctuations at various angular scales with the corresponding observations. However, as shown in Table 1, these predictions can not distinguish the string model from models based on inflation. A potentially interesting way that can lead to this distinction between models is the study of the non-gaussian character of string induced fluctuations. Before discussing a simple model that can lead to the identification of this non-gaussian character I will give a brief introduction to some statistics basics[116] that will be used later.

A pattern of fluctuations of a random variable  $\delta$  is characterized by the probability distribution  $P(\delta)$  that gives the probability that a value  $\delta$  will be detected after a random sampling of the pattern. The  $n^{th}$  moment of the distribution  $P(\delta)$  is defined as

$$<\delta^n> \equiv \int d\delta \ \delta^n P(\delta)$$
 (124)

The most useful moments are  $\mu \equiv <\delta >$  (the mean),  $\sigma^2 = <\delta^2 >$  (the variance),  $a_3 \equiv \frac{<\delta^3>}{\sigma^3}$  (the skewness) and  $a_4 \equiv \frac{<\delta^4>}{\sigma^4}$  (the kurtosis). A distribution is completely defined by its infinite set of moments.

The moment generating function is a very useful function that can produce by differentiation all the moments of a distribution. It is defined as

$$M_{\delta}(t) \equiv \int d\delta \ e^{t\delta} P(\delta) \tag{125}$$

From this definition it immediately follows that

$$\langle \delta^n \rangle = \frac{d^n}{dt^n} M(t)|_{t=0} \tag{126}$$

An interesting example is the gaussian distribution defined as

$$P(\delta) = \frac{1}{\sqrt{2\pi\sigma^2}} e^{-\frac{(\delta-\mu)^2}{2\sigma^2}} \to P(\delta') = \frac{1}{\sqrt{2\pi}} e^{-\frac{\delta'^2}{2}}$$
 (127)

where  $\delta' \equiv \frac{\delta - \mu}{\sigma}$  is a *standardized* random variable. The generating function corresponding to the standardized gaussian distribution is obtained from Eq. (127) and Eq. (125)

$$M_{\delta'}(t) = e^{t^2/2} \Rightarrow a_3 = 0, \qquad a_4 = 3$$
 (128)

A particularly useful theorem that will be used below states that the moment generating function of a sum of two independent random variables is the product of the generating functions corresponding to each variable

$$M_{\delta_1 + \delta_2} = M_{\delta_1} M_{\delta_2} \tag{129}$$

Another basic theorem of statistics is the Central Limit Theorem (hereafter CLT) which states that the sum  $\delta_n = x_1 + ... + x_n$  of a large number of independent random variables  $x_i$  with identical distributions  $P(x_i)$  has a probability distribution that approaches the gaussian in the limit of  $n \to \infty$ .

The above concepts apply in an interesting way to the CMB temperature fluctuations. The primordial fluctuations produced during inflation are due to the quantum fluctuations of an almost free scalar field. Therefore they may be represented as a Fourier series where the phase of each mode is random and uncorrelated with others *i.e.* 

$$\delta = \frac{\delta T}{T}(\theta) \sim \sum_{k} |\delta_k| e^{i\theta_k} e^{ikx}$$
 (130)

where  $\theta_k$  is a random phase. Therefore, since  $\delta$  is a sum of an infinite number of random variables, by the CLT it will obey gaussian statistics.

The CMB fluctuation pattern induced by cosmic strings may be expressed as a superposition of seed functions as in Eq. (110). In what follows I will focus on the KS term and find the probability distribution  $P(\delta)$  of fluctuations induced by this term[107, 118, 119, 120]. The result obtained in this way will only be an upper bound to the non-gaussian character of fluctuations because by the CLT any additional random effect can only make the fluctuations more gaussian.

Consider a step function perturbation with spatial size  $2\Psi$  superposed at a random position on a pixel lattice with size 2L with periodic boundary conditions. The probability that the temperature of a pixel will be shifted positively (negatively) after this superposition is  $p = \frac{\Psi}{L} \ (p = \frac{\Psi}{L})$ . Thus the moment generating function of the fluctuation probability distribution after this single superposition is

$$M_{x_1}(t) = \langle e^{tx_1} \rangle = (pe^t + pe^{-t} + (1-2p))$$
 (131)

The corresponding result after the superposition of n seed functions at random positions is

$$M_{\delta_n \equiv x_1 + \dots + x_n} = (2p \cosh t + (1 - 2p))^n \tag{132}$$

where use of the theorem (129) was made. Assuming small t (since to get the moments we set t = 0 after differentiation) and p while taking large n we may write

$$M_{\delta_n} \simeq (1 + \frac{(2pn)t^2}{2n})^n \to e^{\sigma t^2/2}$$
 (133)

where  $\sigma^2 \equiv 2pn$  is the variance of the gaussian distribution obtained (as expected by the CLT) for a large number n of superposed seeds.

The moments of the distribution may now be easily obtained from Eq. (132) with the help of Eq. (126) as

$$\sigma^2 = \frac{d^2}{dt^2} M_{\delta}(t)|_{t=0} = 2np \tag{134}$$

$$a_3 = \frac{d^3}{dt^3} M_{\delta}(t)|_{t=0} = 0$$
 (135)

$$a_4 = \frac{d^4}{dt^4} M_{\delta}(t)|_{t=0} = 3 + \frac{1 - 6p}{2np} \to 3$$
 (136)

and the gaussian value of the kurtosis is approached as 1/n. Clearly the crucial quantity that determines how close we are to the gaussian probability distribution is the product np. By setting  $p = \frac{\Psi}{L}$  and  $n = M \frac{L}{\Psi}$  (number of seeds per horizon times the number of horizons in the lattice) we obtain  $np = M \simeq 10$ . With this value, the relative deviation of the kurtosis from the gaussian is

$$\frac{a_4 - a_4^{gaussian}}{a_4} \lesssim \frac{1/2M}{3} \simeq \frac{1}{60} \ll 1$$
 (137)

and any non-gaussian feature is undetectable. Can np be decreased in order to amplify the non-gaussian features of the pattern? Clearly, in order to change n we would have to change the model under study since n is determined by the scaling solution whose parameters are fixed for cosmic strings. In order to change p we would only have to change the type of seed function. This is indeed possible by considering the probability distribution of the temperature of a linear (or non-linear) combination of neighboring pixels. The most convenient combination is the temperature difference of neighboring pixels since this leads (for step-like temperature seeds) to a very localized seed function of  $\delta$ -function type. The number of affected pixels (and therefore p) is minimized by such a seed function. Let us therefore calculate the moment generating function corresponding to the variable  $d \equiv \delta^{i+1} - \delta^i$  where the superscript now denotes pixel location. By defining a new probability  $q \equiv \frac{1}{L}$  that a pixel will be affected by a given seed we have (in analogy with Eq. (132))

$$M_{x_1} = \langle e^{tx_1} \rangle = (2qe^t + 2qe^{-t} + qe^{2t} + qe^{-2t} + (1 - 6q))$$
 (138)

and following the same steps as above we can obtain the moments for the new variable d as  $a_3=0$  (due to the symmetry of the seed function) and

$$a_4 = 3 + \frac{1 - 12q}{4nq} \tag{139}$$

But now  $q = \frac{1}{L}$  and  $n = M \frac{L}{\Psi}$  which implies

$$nq \sim \frac{M}{\Psi} \ll M = np$$
 (140)

and the relative deviation of the kurtosis from the gaussian is

$$\frac{a_4 - a_4^{gaussian}}{a_4} \simeq \frac{\Psi/4M}{3} = \frac{\Psi}{12M} \gg \frac{1}{6M}$$
 (141)

The above described test based on the CMB temperature gradient is effective if the the number of pixels  $\Psi$  affected by half the step function is much larger than 2 (see Eq. (141)). Therefore we require

$$\Psi \equiv \frac{\Psi^0}{\delta\Theta_{pix}^0} > \frac{\Psi_{min}^0}{\delta\Theta_{pix}^0} \simeq \frac{2^0}{\delta\Theta_{pix}^0} \gg 2$$
 (142)

where  $\delta\Theta_{pix}^0$  is the pixel size in degrees. Thus the statistics of the temperature gradient patterns provide a more sensitive test for non-gaussianity than statistics of temperature patterns[117, 118] in experiments with resolution of  $\delta\Theta_{pix}^0 \simeq 1^0$  or better.

A more detailed analytical study of the moments of the string induced CMB fluctuations taking into account the growth of the seed functions as the horizon expands may be found in Refs. [118, 107] Those analytical results can be tested by using Monte Carlo simulations performed as follows: A one dimensional array of 512 initially unperturbed pixels is considered and a number  $N = M \frac{512}{\Psi_{min}}$  of step-like seeds ( $\Psi_{min}$  is the initial seed size in units of pixel size which is determined by the resolution of the simulated experiment) is superposed on the array at random positions and with periodic boundary conditions. To simulate the growth of the horizon a larger seed size  $\Psi = \alpha \Psi_{min}$  is considered next and the superosition is repeated for Q such steps until the seed size becomes much larger than the size of the array of pixels (larger seeds shift the whole lattice by a constant and do not affect the statistics). The resulting pattern is then Fourier transformed and gaussianized by assigning random phases to the Fourier modes and reconstructing the pattern. The gaussian and the stringy patterns are then compared using different statistical tests, various resolutions and adding random gaussian noise of various signal to noise ratios. The Monte Carlo pattern constructed along the above lines may be written as

$$\frac{\delta T}{T}(\theta)|_{str} = \sum_{q=1}^{Q} \sum_{i=1}^{N/\alpha^q} a_n f_1^{\alpha^q \Psi}(\theta - \theta_i)$$
(143)

while the Fourier transform is obtained as

$$\frac{\tilde{\delta T}}{T}(k) = \frac{1}{2L} \int_{-L}^{L} d\theta e^{ik\pi\theta/L} \frac{\delta T}{T}(\theta)|_{str}$$
 (144)

and the gaussianized pattern with the same scale invariant power spectrum is

$$\frac{\delta T}{T}(\theta)|_{gauss} = \sum_{k=-\infty}^{+\infty} |\frac{\tilde{\delta T}}{T}(k)| e^{i\theta_k} e^{ik\pi\theta/L}$$
(145)

where  $\theta_k$  is a random phase.

Figure 16: An exaggerated stringy temperature CMB pattern composed of temperature Kaiser-Stebbins discontinuities(a) compared with its random phase realization (b) (Ref. [119]).

Figure 17: Plot of kurtosis of temperature fluctuations versus angular resolution  $(\theta_{min})$  with zero noise. Even at the lowest resolutions ( $\sim 0.5 arcmin$ ), this test cannot distinguish the gaussian from the string pattern (Ref. [119]).

Fig. 16a demonstrates a stringy pattern with unrealistically amplified non-gaussian features (small number of seeds, fixed seed size) while Fig. 16b is the corresponding gaussianised (random phase pattern). These two types of patterns may now be compared using statistical tests based on the moments of the distributions. After constructing 100 realizations in each case, the mean and standard deviation (cosmic variance of string perturbations[121]) of the kurtosis is found for various experimental resolutions starting from 0.5 arcmin to one degree. Even without noise added this test proves inadequate to identify the non-gaussian features of the stringy pattern (Fig. 17).

This could have been expected in view of the above analytical considerations. The corresponding test for the temperature difference of neighboring pixels however is much more efficient as shown in Fig. 18a where the kurtosis of the two types of patterns are compared. For resolutions better than a few arcminutes the non-gaussian features of the stringy pattern are manifest through a significant increase of the kurtosis.

Figure 18: Plot of kurtosis of temperature gradient of fluctuations versus angular resolution. For small resolutions and zero noise (a), this test can distinguish between seed and gaussian patterns. With gaussian instrumental noise added (b) noise to signal ratio of n/s = 0.3 destroys all trace of the non-gaussian features of the seed pattern. The signal survives at  $n/s \approx 0.1$  (Ref. [119]).

Unfortunately this nice feature of this test is very sensitive to the addition of noise to the fluctuation pattern as shown in Fig. 18b which shows the effect of adding a modest amount of noise (the noise to signal ratio was n/s = 0.3) on the kurtosis of the temperature difference pattern. This sensitivity to noise of the temperature difference patterns is due to the low temperature derivative for most pixels in temperature patterns constructed by step-function superposition compared to the much larger derivative of noise patterns. Thus it is much easier for noise to dominate in temperature difference (derivative) patterns.

### 7 Conclusion

The purpose of this review was to give an introduction to the basic features of the cosmic string model for large scale structure formation and to show some of the recent developments in testing the model by comparing with new detailed observational data. The main points stressed are the following:

- 1. Cosmic strings are linear concentrations of trapped energy predicted by GUTs to form during a phase transition in the early universe.
- 2. For a natural value of a single free parameter  $\mu$  (mass per unit length) strings may provide the seeds for structure formation.
- 3. The main achievements of the model include the following
  - Three independent types of requirements lead to the same value for the free parameter  $\mu$  of the model: Large Scale Structure, Microwave Background, Grand Unified Theories.
  - There is a well defined mechanism for the formation of the observed sheets and filaments of galaxies on large scales.
  - The model can resurrect massive neutrinos as dark matter candidates since strings+HDM appears to be a viable model for structure formation with amplified power on large scales (seeds survive free streaming).
  - The statistics and power spectrum of the predicted CMB fluctuations are consistent with current CMB observational data.

- The existence of a scaling solution makes the model consistent with standard cosmology in contrast with other models based on topological defects.
- 4. The main challenges of the model include the following
  - The complexity of performing detailed simulations of structure formation including both the string network and matter. This results to a large uncertainty in the predictions of the model.
  - The  $L^{-1}$  scaling of the predicted velocity fields with scale L is hard to reconcile with large scale velocity field observations.
  - The msec pulsar constraints appear to uncomfortably close to ruling out the model.

The model makes some well defined unique predictions that can be used to rule out or verify it

- The CMB fluctuations are predicted to have certain non-gaussian features on scales of 1' or smaller.
- The model predicts the concentration of multiple images of lensed objects in small areas in the sky with certain unique characteristics. Such an event may have already been detected.

#### Acknowledgements

It is a pleasure to thank Qaisar Shafi and all the organizers of the Trieste Summer School for an invitation to lecture at an exciting and well organized school. This work was supported by a CfA Postdoctoral fellowship and by DOE Grant DE-FG0291ER40688, Task A.

## References

- [1] see e.g., S. Weinberg, 'Gravitation and Cosmology' (Wiley, New York, 1972).
- [2] E. Milne, Zeits. f. Astrophys. 6, 1 (1933).

- [3] J. Mather et al., Ap. J. (Lett.) **354**, L37 (1990).
- [4] E. Hubble, Proc. Nat. Acad. Sci. 15, 168 (1927).
- [5] R. Partridge, Rep. Prog. Phys. **51**, 647 (1988).
- [6] A. Penzias and R. Wilson, Ap. J. 142, 419 (1965).
- [7] D. Fixen, E. Cheng and D. Wilkinson, *Phys. Rev. Lett.* **50**, 620 (1983).
- [8] R. Alpher and R. Herman, Rev. Mod. Phys. 22, 153 (1950)
   G. Gamov, Phys. Rev. 70, 572 (1946).
- [9] R. Dicke, P.J.E. Peebles, P. Roll and D. Wilkinson, Ap. J. 142, 414 (1965).
- [10] R. Alpher, H. Bethe and G. Gamov, *Phys. Rev.* 73, 803 (1948)
   R. Alpher and R. Herman, *Nature* 162, 774 (1948).
- [11] S. Shechtman, P. Schechter, A. Oemler, D. Tucker, R. Kirshner and H. Lin, Harvard-Smithsonian preprint CFA 3385 (1992), to appear in 'Clusters and Superclusters of Galaxies', ed. by A. Fabian (Kluwer, Dordrecht, 1993)
  S. Shechtman et al., 'The Las Campanas Fiber-Optic Redshift Survey', CFA preprint (1994), to be publ. in the proc. of the 35th Herstmonceaux Conference "Wide Field Spectroscopy and the Distant Universe".
- [12] Ya.B. Zel'dovich, J. Einasto and S. Shandarin, Nature 300, 407 (1982)
  J. Oort, Ann. Rev. Astron. Astrophys. 21, 373 (1983)
  R.B. Tully, Ap. J. 257, 389 (1982)
  S. Gregory, L. Thomson and W. Tifft, Ap. J. 243, 411 (1980).
- [13] N. Bahcall and R. Soneira, Ap. J. 270, 20 (1983)
  A. Klypin and A. Kopylov, Sov. Astr. Lett. 9, 41 (1983).
- [14] V. de Lapparent, M. Geller and J. Huchra, Ap. J. (Lett) 302, L1 (1986).
- [15] M. Davis and J. Huchra, Ap. J. 254, 437 (1982).
- [16] V. Trimble, Ann. Rev. Astr. Astrophys. 25, 423 (1987).

- [17] E. Bertschinger and A. Dekel, Ap. J. 336, L5 (1989).
- [18] M. Strauss, M. Davis, A. Yahil and J. Huchra, Ap. J. 385, 421 (1992).
- [19] J. Primack, D. Seckel and B. Sadoulet, Ann. Rev. Nucl. Part. Sci. 38, 751 (1988).
- [20] J. Preskill, M. B. Wise and F. Wilczek, *Phys. Lett.* **B120**, 127 (1983).
- [21] J. Bond, G. Efstathiou and J. Silk, *Phys. Rev. Lett.* 45,(1980)
   J. Bond and A. Szalay, *Ap. J.* 274, 443 (1983).
- [22] W. Press, *Phys. Scr.* **21**, 702 (1980).
- [23] G. Chibisov and V. Mukhanov, 'Galaxy Formation and Phonons,' Lebedev Physical Institute Preprint No. 162 (1980)
  G. Chibisov and V. Mukhanov, Mon. Not. R. Astron. Soc. 200, 535 (1982).
- [24] V. Lukash, Pis'ma Zh. Eksp. Teor. Fiz. 31, 631 (1980).
- [25] K. Sato, Mon. Not. R. Astron. Soc. 195, 467 (1981).
- [26] A. Guth, *Phys. Rev.* **D23**, 347 (1981).
- [27] T.W.B. Kibble, J. Phys. A9, 1387 (1976).
- [28] T.W.G. Kibble, *Phys. Rep.* **67**, 183 (1980).
- |29| A. Vilenkin, Phys. Rep. **121**, 263 (1985).
- [30] N. Turok, 'Phase Transitions as the Origin of Large-Scale Structure,' in 'Particles, Strings and Supernovae' (TASI-88) ed. by A. Jevicki and C.-I. Tan (World Scientific, Singapore, 1989).
- [31] A. Vilenkin and E.P.S. Shellard, 'Strings and Other Topological Defects' (Cambridge Univ. Press, Cambridge, 1994).
- [32] see e.g., G. Ross, Grand Unified Theories (Benjamin, Reading, 1985).
- [33] G. Blumenthal, S. Faber, J. Primack and M. Rees, *Nature* 311, 517 (1984)
  M. Davis, G. Efstathiou, C. Frenk and S. White, *Ap. J.* 292, 371 (1985).

- [34] Ya.B. Zel'dovich, Mon. Not. R. astron. Soc. 192, 663 (1980).
- [35] A. Vilenkin, Phys. Rev. Lett. 46, 1169 (1981).
- [36] N. Steenrod, 'The topology of fibre bundles' Princeton Univ. Press. (1951).
- [37] L. Perivolaropoulos *Phys. Lett.* **B316**, 528 (1993) and references therein.
- [38] T. Vachaspati, Nucl. Phys. B397 (1993).
  M. James L. Perivolaropoulos and T. Vachaspati, Phys. Rev. D46, R5232 (1992).
  M. James L. Perivolaropoulos and T. Vachaspati, Bulletin Board: hep-ph@xxx.lanl.gov 9212301, Nucl. Phys. B395, 534 (1993).
  A. Achucarro, K. Kuijken L. Perivolaropoulos and T. Vachaspati, Nucl. Phys. B388, 435 (1992).
- [39] D. Mermin, Rev. Mod. Phys. **51**, 591 (1979).
- [40] P. de Gennes, 'The Physics of Liquid Crystals' (Clarendon Press, Oxford, 1974)
  I. Chuang, R. Durrer, N. Turok and B. Yurke, Science 251, 1336 (1991)
  M. Bowick, L. Chandar, E. Schiff and A. Srivastava, Science 263, 943 (1994).
- [41] M. Salomaa and G. Volovik, Rev. Mod. Phys. **59**, 533 (1987).
- [42] A. Abrikosov, *JETP* 5, 1174 (1957).
- [43] R. Davis, *Phys. Rev.* **D35**, 3705 (1987).
- [44] N. Turok, Phys. Rev. Lett. **63**, 2625 (1989).
- [45] G. H. Derrick, J. Math. Phys. 5, 1252 (1964).
- [46] see e.g. R. Rajaraman, 'Solitons and Instantons', North Holland Publishing (1987), p. 78, and references therein.
- [47] L. Perivolaropoulos, *Phys. Rev.* **D46**, 1858 (1992).
- [48] T. Prokopec, A. Sornborger and R. Brandenberger, *Phys. Rev.* **D45**, 1971 (1992).

- [49] J. Borrill, E. Copeland and A. Liddle, *Phys. Lett.* **258B**, 310 (1991).
- [50] A. Sornborger, Phys. Rev. **D48**, 3517 (1993).
- [51] N. Turok and D. Spergel, Phys. Rev. Lett. 64, 2736 (1990).
- [52] A. Gooding, D. Spergel and N. Turok, Ap. J. (Lett.) 372, L5 (1991)
  C. Park, D. Spergel and N. Turok, Ap. J. (Lett.) 373, L53 (1991).
- [53] D. Spergel, N. Turok, W. Press and B. Ryden, Phys. Rev. D43, 1038 (1991).
- [54] R. Cen, J. Ostriker, D. Spergel and N. Turok, Ap. J. 383, 1 (1991).
- [55] N. Turok, *Phys. Scripta* **T36**, 135 (1991).
- [56] H. Nielsen and P. Olesen, Nucl. Phys. **B61**, 45 (1973).
- [57] M. Barriola and A. Vilenkin, *Phys. Rev. Lett.* **63**, 341 (1989).
- [58] S. Rhie and D. Bennett, Phys. Rev. Lett. 65, 1709 (1990).
- [59] L. Perivolaropoulos, Bulletin Board: hep-ph@xxx.lanl.gov 9207255, Mod. Phys. Lett. A7 903 (1992).
- [60] L. Perivolaropoulos, Bulletin Board: hep-ph@xxx.lanl.gov 9310264, Phys. Rev. D48, 5961 (1993).
- [61] W. Perkins, L. Perivolaropoulos, R. Brandenberger, A. C.Davis and A. Matheson, Nucl. Phys. B353 237 (1991) and references therein.
  R. Brandenberger and L. Perivolaropoulos, Phys. Lett. 208B 396 (1988).
  A. Matheson, R. Brandenberger, A. C.Davis, and L. Perivolaropoulos and W. Perkins, Phys. Lett. 248B 263 (1990).
- [62] T. Vachaspati and A. Vilenkin, Phys. Rev. **D30**, 2036 (1984).
- [63] D. Foerster, Nucl. Phys. **B81**, 84 (1974).
- [64] N. Turok, in 'Proceedings of the 1987 CERN/ESO Winter School on Cosmology and Particle Physics' (World Scientific, Singapore, 1988).
- [65] E.P.S. Shellard, Nucl. Phys. **B283**, 624 (1987).

- [66] R. Matzner, Computers in Physics 1, 51 (1988) K. Moriarty, E. Myers and C. Rebbi, Phys. Lett. 207B, 411 (1988)
  E.P.S. Shellard and P. Ruback, Phys. Lett. 209B, 262 (1988).
- [67] L. Perivolaropoulos Nucl. Phys. **B375** 655 (1992).
- [68] P. Ruback, Nucl. Phys. **B296**, 669 (1988).
- [69] T. Vachaspati and A. Vilenkin, Phys. Rev. **D31**, 3052 (1985)
   N. Turok, Nucl. Phys. **B242**, 520 (1984)
  - C. Burden, Phys. Lett. 164B, 277 (1985).
- [70] A. Albrecht and N. Turok, *Phys. Rev. Lett.* **54**, 1868 (1985).
- [71] D. Bennett and F. Bouchet, *Phys. Rev. Lett.* **60**, 257 (1988).
- [72] B. Allen and E.P.S. Shellard, *Phys. Rev. Lett.* **64**, 119 (1990).
- [73] A. Albrecht and N. Turok, *Phys. Rev.* **D40**, 973 (1989).
- [74] B. Carter, Phys. Rev. **D41**, 3869 (1990).
- [75] E. Copeland, T.W.B. Kibble and D. Austin, *Phys. Rev.* **D45**, 1000 (1992).
- [76] D. Vollick, Phys. Rev. **D45**, 1884 (1992)
- [77] T. Vachaspati and A. Vilenkin, *Phys. Rev. Lett.* **67**, 1057 (1991).
- [78] Ya.B. Zel'dovich and M. Khlopov, Phys. Lett. 79B, 239 (1978)
   J. Preskill, Phys. Rev. Lett. 43, 1365 (1979).
- [79] P. Langacker and S.-Y. Pi, *Phys. Rev. Lett.* **45**, 1 (1980).
- [80] Ya.B. Zel'dovich, I. Kobzarev and L. Okun, Zh. Eksp. Teor. Fiz. 67, 3 (1974).
- [81] A. Vilenkin, Phys. Rev. **D23**, 852 (1981)
  - J. Gott, Ap. J. 288, 422 (1985)
  - W. Hiscock, *Phys. Rev.* **D31**, 3288 (1985)
  - B. Linet, Gen. Rel. Grav. 17, 1109 (1985)
  - D. Garfinkle, *Phys. Rev.* **D32**, 1323 (1985)
  - R. Gregory, Phys. Rev. Lett. 59, 740 (1987).

- [82] N. Kaiser and A. Stebbins, *Nature* 310, 391 (1984)
  A. Stebbins, *Astrophys. J.* 327, 584 (1988).
- [83] R. Gott 1985, Ap. J. 288, 422.
- [84] C. Hogan and R. Narayan, M.N.R.A.S., **211** 575 (1984).
- [85] N. Turok, Nucl. Phys. **B242**, 520 (1984).
- [86] T. Vachaspati, Phys. Rev. Lett. 57, 1655 (1986).
- [87] J. Silk and V. Vilenkin, Phys. Rev. Lett. 53, 1700 (1984).
- [88] A. Stebbins, S. Veeraraghavan, R. Brandenberger, J. Silk and N. Turok, Ap. J. **322**, 1 (1987).
- [89] R. Brandenberger, L. Perivolaropoulos and A. Stebbins, Int. J. of Mod. Phys. A5, 1633 (1990)
  L. Perivolaropoulos, R. Brandenberger and A. Stebbins, Phys. Rev. D41, 1764 (1990)
  R. Brandenberger, Phys. Scripta T36, 114 (1991).
- [90] T. Hara and S. Miyoshi, Ap. J. 405, 419 (1993).
- [91] N. Turok and R. Brandenberger, Phys. Rev. D33, 2175 (1986)
  A. Stebbins, Ap. J. (Lett.) 303, L21 (1986)
  H. Sato, Prog. Theor. Phys. 75, 1342 (1986).
- [92] S. White, C. Frenk and M. Davis, Ap. J. (Lett.) 274, L1 (1983).
- [93] R. Brandenberger, N. Kaiser, D. Schramm and N. Turok, Phys. Rev. Lett. 59, 2371 (1987).
- [94] R. Brandenberger, N. Kaiser and N. Turok, Phys. Rev. D36, 2242 (1987).
- [95] T. Vachaspati Phys. Lett. B282 305, (1992).
  L. Perivolaropoulos and T. Vachaspati, Bulletin Board: hep-ph@xxx.lanl.gov 9303242, Ap. J. Lett. 423, L77 (1994).
- [96] E. Harrison, Phys. Rev. D1, 2726 (1970) Ya.B. Zel'dovich, Mon. Not. R. astron. Soc. 160, 1p (1972).

- [97] A. Guth and S.-Y. Pi, Phys. Rev. Lett. 49, 1110 (1982)
  - S. Hawking, *Phys. Lett.* **115B**, 295 (1982)
  - A. Starobinsky, *Phys. Lett.* **117B**, 175 (1982)
  - R. Brandenberger and R. Kahn, Phys. Rev. D28, 2172 (1984)
  - J. Frieman and M. Turner, *Phys. Rev.* **D30**, 265 (1984)
  - V. Mukhanov, *JETP Lett.* **41**, 493 (1985).
- [98] A. Albrecht and A. Stebbins, *Phys. Rev. Lett.* **68**, 2121 (1992).
- [99] A. Albrecht and A. Stebbins, *Phys. Rev. Lett.* **69**, 2615 (1992).
- [100] C.J. Hogan and M.J. Rees, Nature 311, 109 (1984).
  B. Bertoti, B.J. Carr and M.J. Rees, M.N.R.A.S. 203, 945 (1983).
  F.R. Bouchet, D.P. Bennett, Phys. Rev. D41, 720 (1990).
- [101] R.R. Caldwell and B. Allen, *Phys. Rev.* **D45** 3447, (1992).
- [102] D.R. Stinebring, M.F. Ryba, J.H. Taylor (Princeton U.) and R.W. Romani, *Phys.Rev.Lett.* **65** 285 (1990).
- [103] L. L. Cowie and E. M. Hu, Ap. J. 318 L33 (1987).
   E.M. Hu, Ap. J. 360, L7 (1990).
- [104] J.N. Hewitt, R.A. Perley, E.L. Turner and E.M. Hu, *Ap. J.* **356**, 57 (1990).
- [105] see e.g., G. Efstathiou, in 'Physics of the Early Universe,' proc. of the 1989 Scottish Univ. Summer School in Physics, ed. by J. Peacock, A. Heavens and A. Davies (SUSSP Publ., Edinburgh, 1990).
- [106] L. Perivolaropoulos, *Phys. Lett.* **298B**, 305 (1993).
- [107] L. Perivolaropoulos, Bulletin Board: hep-ph@xxx.lanl.gov 9403298, Phys. Rev. **D50** 962 (1994).
- [108] A. R. Liddle, D. H. Lyth, The Spectral Slope in the Cold Dark Matter Cosmogony, Bulletin Board: astro-ph@babbage.sissa.it - 9209003, SUSSEX-AST-92-8-1, (1992).
- [109] R. Sachs and A. Wolfe, Ap. J. 147, 73 (1967).

- [110] T. Padmanabhan, 'Structure Formation in the Universe' (Cambridge Univ. Press 1993).
- [111] L. Perivolaropoulos, Spectral Analysis of Microwave Background Perturbations Induced by Cosmic Strings, Bulletin Board: astro-ph@babbage.sissa.it 9402024, CfA-3796, submitted to Ap. J. (1994).
- [112] D. Bennett, A. Stebbins and F. Bouchet, Ap. J. (Lett.) 399, L5 (1992).
- [113] D. Bennett, F. Bouchet and A. Stebbins, *Nature* **335** 410 (1988).
- [114] COBE: G. Smoot et al., Ap. J. (Lett.) 396, L1 (1992).
  MSAM: S. Meyer, E. Cheng and L. Page, Ap. J. (Lett.) 371, L7 (1991)
  MSAM: K. Ganga, E. Cheng, S. Meyer and L. Page, Ap. J. (Lett.) 410, L57 (1993).
  - S. Hancock et al., *Nature* **317**, 333 (1994).
  - SK: E. Wollack et al., Ap. J. (Lett.) 419, L49 (1993).
  - SP91: T. Gaier et al., Ap. J. (Lett.) 398, L1 (1992)
  - SP91: J. Schuster et al., Ap. J. (Lett.) 412, L47 (1993).
  - P. de Bernardis et al., Ap. J. (Lett.) 422, L33 (1994).
  - M. Dragovan et al., Princeton preprint (1993).
  - MAX: P. Meinhold et al., Ap. J. (Lett.) 409, L1 (1993).
  - MAX: J. Gunderson et al., Ap. J. (Lett.) 413, L1 (1993).
  - E. Cheng et al., Ap. J. (Lett.) **422**, L37 (1994).
  - WD: G. Tucker, G. Griffin, H. Nguyen and J. Peterson, *Ap. J.* (*Lett.*) **419**, L45 (1993).
  - OVRO: A. Readhead et al., Ap. J. **346**, 566 (1989).
  - S. Myers, A. Readhead and A. Lawrence, Ap. J. 405, 8 (1993).
- [115] R. Bond, R. Crittenden, R. Davis, G. Efstathiou and P. Steinhardt, Phys. Rev. Lett. **72**, 13 (1994).
- [116] W. Feller, 'An Introduction to Probability Theory and its Applications', New York: Willey, (1971).
- [117] J.R.Gott III, C. Park, R. Juszkiewicz, W. Bies, D. Bennett, F. Bouchet, A. Stebbins, Ap. J. 352, 1 (1990).
- [118] R. Moessner, L. Perivolaropoulos and R. Brandenberger, Bulletin Board: astro-ph@babbage.sissa.it 9310001, Ap. J. 425, 365 (1994).

- [119] A. Gilbert and L. Perivolaropoulos, CfA preprint, submitted to Astroparticle Physics (1994).
- [120] L. Perivolaropoulos, M.N.R.A.S. **267**, 529 (1994).
- [121] A. Gangui and L. Perivolaropoulos, CFA-3915, Submitted to Astrophys. J. Bulletin Board: astro-ph@babbage.sissa.it 9408034, (1994).

This figure "fig1-1.png" is available in "png" format from:

This figure "fig2-1.png" is available in "png" format from:

This figure "fig1-2.png" is available in "png" format from:

This figure "fig2-2.png" is available in "png" format from:

This figure "fig1-3.png" is available in "png" format from:

This figure "fig2-3.png" is available in "png" format from: